Journal of Engineering Physics and Thermophysics, Vol. 72, No. 6, 1999

REVIEWS

PENETRATION OF LARGE METEOROIDS INTO THE ATMOSPHERE: THEORY AND OBSERVATIONS

I. V. Nemchinov, O. P. Popova, and
A. V. Teterev

UDC 523.68

Introduction. Impacts of space bodies that bombard planets surrounded by an atmosphere largely govern the evolution of their surface and the atmosphere itself and, for the earth, its biosphere. When a meteoroid enters the atmosphere complex aerodynamic and physical-gasdynamic processes occur: hypersonic flow, ablation, the radiation of atmospheric gas heated in shock waves (in what follows, for all planets, this gas will be referred to as simply air); the formation of a vapor and an air–vapor mixture and their radiation, chemical reactions in air and the vapor, and, finally, breakup of the body itself and its fragments. These processes in turn govern the rate of removal of the space-body mass, retardation, energy release in air, the intensity of shock waves, luminous fluxes, etc. and ultimately affect the character and degree of the hazard to mankind due to asteroids and comets [1, 2].

A special feature of the physical-gasdynamic processes that occur upon entry of meteoroids, as compared to processes investigated in detail that accompany the entry of man-produced objects (forebodies of rockets, space probes, and others) into the atmosphere is that the average velocity of the former is much higher. Therefore the plasma temperatures and the radiation fluxes turn out to be much higher. The latter is a dominant factor and not a correction to the heat fluxes determined by ordinary (molecular or electronic) heat conduction and turbulent heat transfer. A second significant factor is intense breakup of meteoroids in the atmosphere under the action of comparatively low aerodynamic forces, it often being multiple. Third, the dimensions of the large meteoroids under consideration are sometimes larger than the dimensions of the indicated objects and a change in the optical thicknesses of the air and vapor plasmas affects both the magnitude of the radiation fluxes and their spectra. Meteoroid material is very different from the heatproof coatings of the indicated objects – meteoroids evaporate much more easily and sometimes lose a great deal of mass due to the blowing-away of a liquid film, which increases both the mass losses and the radiation fluxes.

A theoretical analysis of the processes of entry into the atmosphere is hindered further by the fact that the properties of the meteoroids themselves (composition, density, shape, strength, and structure) and the probability of their fall are unknown or, in any case, are poorly known. These data are accumulated gradually in studying data on craters on the surfaces of planets and their satellites and in astronomical observations of space bodies outside the atmosphere. Important information is provided by analysis of meteorites (the remains of meteoroids fallen onto the surface). Observations of meteors, i.e., phenomena in the atmosphere induced by the entry of meteoroids into it, permit determination of the trajectory, the light curve of the meteor, sometimes the radiation spectrum, etc.

Earlier, in the Seventies and Eighties, there were three ground observation networks – the Prairic (the events are marked by the index PN), Canadian (MORP), and European (EN) Networks. Now, there is only one functioning network – the European Observation Network [3-5]. It consists of 34 photometric chambers, each covering approximately 100 km with its field of view. On the whole, they cover about 10^6 km^2. The network performs approximately 10,000 exposures a year, i.e., about 1200 hours of observations are carried out in a clear sky (3 hours a day, on average) [5]. In recent years, the network has recorded bolides, i.e., meteors brighter than

Institute of the Dynamics of the Geospheres, Russian Academy of Sciences, Moscow, Russia. Translated from Inzhenerno-Fizicheskii Zhurnal, Vol. 72, No. 6, pp. 1233-1265, November–December, 1999. Original article submitted March 5, 1999.

 1062-0125/99/7206-1194$22.00

-6^{mag}, with a frequency of 50 per year. We point out that the brightness m_v corresponds to the radiation intensity $I = I_0 \cdot 10^{-0.4m_v}$, where I is usually determined in the sensitivity range of a panchromatic film used commonly in ground observations, while $I_0 = 830$ W [3].

In the past four decades the European Network has recorded 23 bolides that could be accompanied by the fall of meteorites of rather large mass. Only one meteorite (Pŷibram) has been found [6]. Of the meteorites recorded by the Prairic Network, the Lost City meteorite was found [7], and of the meteorites recorded by the Canadian Network the Innisfree was found [8]. This small number of meteorites found is due to the fact that meteoroids break up in the atmosphere under the action of aerodynamic loads, usually at significant heights [9]. Large fragments, continuing to move with a high velocity, sometimes break up several more times [9, 10], and small fragments are retarded rather quickly and also evaporate. In this case, meteoric material, if reaches the earth, does so mainly in the form of fine meteoric dust. Only occasionally do fragments of bodies of comparatively low initial velocities and a moderately large initial dimension manage to be retarded, cease to evaporate and to break up, and fall out in the form of meteorites.

The number of fragments recorded in flight was 6 in Innisfree and 17 for Pŷibram. According to evaluations [11] of the dynamic mass between intense breakups, meteoroid PN 40590 lost 42% of its mass in the process of fragmentation at a height of 40 km, 10% at a height of 30 km, and most of the remaining mass at a height of 23 km. The Lost City meteorite turned out to be an N-chondrite and had a mass of 17 kg for an initial mass of about 160 kg (the initial radius was approximately 35 cm).

It can be assumed that some types of meteoroids, namely of cometary origin, that have low strength and a high velocity of entry are not presented in collections of meteorites at all, although ideas of how they could look are formulated [12] and a seach for them is started. Therefore observations on preatmospheric and atmospheric segments of the trajectory are particularly important for these meteoroids.

In this work we will consider the entry, into the atmosphere, of comparatively large meteoroids but not too large – with a size of 1–100 m, i.e., much smaller than those (with a size of 1–10 km) that can induce a global catastrophe and mass disappearance of species on the earth [2, 13, 14]. For very large bodies (1–10 km), the atmosphere has practically no effect all the way to the moment of impact against a solid or water surface of the earth, although its disturbance after impact and the release of a large mass of material are one of the main reasons for the global catastrophe. The program of long-term astronomical observations is aimed at cataloging precisely these very large bodies and determining their orbits and the probability of impact against the earth [15, 16]. However an asteroid hazard can be represented by smaller bodies, namely, with a size of 10–100 m, the hazard growing with the development of civilization [1]. These bodies can be seen in telescopes only when they are passing very close to the earth [17, 18]. Analysis of meteor phenomena induced by the entry of bodies with a size of 0.1–1 m, for which certain rather extensive statistics of observations are available, enables us to assess the probability of fall and to reveal some features of the process of entry of meteoroids into the atmosphere, since the corresponding meteor phenomena are no longer too different in scale from the phenomena for larger (10–100 m) bodies.

As will be shown below, bodies with a size of 100 m and sometimes even smaller pass through the atmosphere to the surface almost without breakup, inducing formation of craters and release of a large amount of dust into the atmosphere [19], seismic effects [1, 20], and tsunami waves [1, 21-23]. The latter factor has attracted close attention in recent years. As is shown, for example, in [24], an asteroid with a radius of 100 m falling into the Pacific Ocean (with a probability of approximately once every 10,000 years) induces a 14–21 m-high tsunami wave in the coastal regions of Japan and Taiwan, near Shanghai, on the Hawaiian Islands, and in other places that are usually heavily populated. Thus, the probability of this catastrophic event occurring in the next century amounts to approximately 1%. Seismic waves can have a destructive effect on chemical plants and nuclear power plants that are rather densely located in individual regions of the earth and on radioactive-waste storage sites even in impact against the surface at a rather large distance from these and other potentially hazardous sites [1].

Investigation of entry into the atmosphere is important since to a large extent the atmosphere protects the earth from direct impacts on its surface, attenuating or eliminating processes of crater formation and seismic effects and decreasing the amplitude of tsunami waves. On the other hand, even on entry into the atmosphere [1, 25, 26]

and the more so in "explosion" of a meteoroid in air low over the earth's surface [1, 27] rather powerful shock waves and radiation fluxes can occur that can cause the destruction of buildings and fires [1, 2], similar in many ways to those from nuclear explosions [28].

Retardation of a Meteoroid and Its Fragmentation. Simple evaluations [1, 29] show that, for large bodies, ablation from the surface is insignificant because of shielding of the surface by the vapor produced, and the mass of the meteoroid or its fragments changes little between fragmentations. The motion of the meteoroid in the atmopshere under the assumption of constancy of its mass M, shape, and cross-sectional area S is described by the equation

$$M\frac{dV}{dt} = -C_D\rho_a\frac{V^2}{2}S. \tag{1}$$

The height is determined by the simple equation

$$\frac{dZ}{dt} = -V\sin\theta. \tag{2}$$

Combining (1) and (2), we obtain

$$\frac{M}{S}\frac{d(V^2)}{dZ} = \frac{C_D\rho_a V^2}{\sin\theta} \tag{3}$$

Integrating (3), we find

$$V^2 = V_B^2\exp\left(-\frac{m_a}{m_0}\frac{1}{\sin\theta}\right), \tag{4}$$

where

$$m_0 = \frac{M}{SC_D},\quad m_a(Z) = \int_Z^{Z_B}\rho_a\,dZ. \tag{5}$$

According to [5], retardation begins only where the specific mass of the atmosphere m becomes comparable to the specific mass of the meteoroid m_0. For a spherical meteoroid with a radius R = 30 m and a density of 1 ton/m^3 (water or ice), we obtain $m_0 = \frac{4}{3}R\rho_0 = 40$ ton/m^2 when $C_D = 1$, while even for the earth's surface ($Z = 0$) the specific mass m_a of the atmospheric column above it is of the order of 10 ton/m^2. Thus, even ice bodies with a radius of about 30 m, the more so stony or iron bodies, would be likely to reach the Earth virtually without retardation, following not only a vertical trajectory but also even a strongly inclined trajectory.

Impacts on the solid surface of the earth lead to formation of craters whose size is roughly of the order of 20 radii of the striker [19], i.e., for a body with a radius of 30–50 m, we are dealing with 0.5–1-km craters. An example is the renowned Meteor Crater formed about 50 thousand years ago in Arizona [19]. Its diameter is 1.2 km and its depth is 180 m. The kinetic energy of the colliding iron body is estimated at 20–40 Mton in TNT equivalent [19]. However, the number of these craters is small because of the low probability of iron bodies falling (according to [30], the number of iron meteoroids amounts to approximately 5% of all meteoroids). Stony and especially cometary bodies have lower strength and with the same initial energy can break up in the atmosphere without reaching the surface. This is indicated by the air character of the explosion of the Tunguska meteoroid on June 30, 1908 [31-33], estimated as having a mass and energy [34] similar to those for the iron meteoroid that caused the formation of Meteor Crater [1, 31, 34, 35]. The explosion in air was produced by strong breakup of the meteoroid in flight, which sharply increased the local intensity of energy release. Traces of low-altitude explosions of meteoroids disappear comparatively rapidly from the surface. This is partially the reason for the great interest in the Tunguska phenomenon of 1908 where these traces are still preserved: the area of the forest's fall

attained 2150 km^2, and there is a "spot" (3–5 km in diameter) of trees standing vertically that resemble telegraph poles. The territory of intense burning of the trees was 200 km^2 at the center of the forest's fall with a quite large area of fires. Had this explosion occurred over a large city it would have been destroyed [28].

The explanation of the characteristic feature of the forest's fall in the Tunguska event ("butterfly") by the interaction of a ballistic wave and a shock wave was given for the first time as a result of a laboratory model experiment with the use of an inclined detonating cord and a concentrated charge on the end [36, 37]. The energy of the Tunguska event [31, 35] was also determined by comparison of calculations [35, 38-40] with the data on the area of the forest's fall [41], thermal-radiation burn [1, 42], and acoustic [43, 44] and seismic signals [44-46]. The height of the "explosion" was estimated at 5–10 km, the analogy with a nuclear explosion being employed [28]. However the "meteoroid explosion" is not "point" and "instantaneous" but is extended in time and space. Therefore the energy estimates themselves are largely related to the selected model of the phenomenon, which in turn depends on the adopted model of the meteoroid and its strength.

The properties of comets are the least clear [47]. There are four basic models of cometary centers, namely, the ice-conglomerate model [48, 49], the fractal model [50], the "rubble-pile" model [51], and, finally, the model of blocks glued together with ice [52]. The density, structure, and composition of comets can vary in accordance with the site of their formation in the solar system and with age. These can exist extinct comets that lost the major portion of the volatile agents as a result of a long journey about the sun. In appearance (by the low albedo and the absence of coma), they are hard to differentiate from asteroids. Finally, galactic comets that arrive in the solar system from outside are, in principle, possible.

As far as the Tunguska phenomenon is concerned, an idea of the trajectory of the Tunguska bolide, its slope, and the velocity, unfortunately, is provided only by scanty and contradictory data of visual observations (see review [33]). The problem of whether the Tunguska event results from the fall of a comet or an asteroid has been discussed up to the present [33, 34, 53-59]. Numerous calculations of the interaction between a shock wave from the explosion of a space body and a ballistic wave induced by its flight [27, 33, 35, 40, 56, 57] left open the issue of what an "explosion" is and in what manner it occurs. It seems that this and many other issues associated with the penetration of meteoroids into the earth's atmosphere cannot be solved by pure theory, in particular, without analyzing the available data on penetration of other bodies, including bodies of smaller dimension, into the atmosphere. Unfortunately, these data are also very scanty for the moment.

Benešov Bolide. Complete data of observations of a bolide (dynamics, brightness, spectrum) are placed at reseachers' disposal very rarely. This information was obtained for the Benešov bolide at the Ondrejov Observatory of the European Bolide Network in 1991 [60]. The meteorite was not found on the earth.

The Benešov bolide (EN 070591) had a rather high initial velocity (V_B = 21 km/sec). It began to be recorded at a height of 90 km (H_B), attained maximum brightness (-19.5^{mag}) at a height of 24 km (H_{max}), and was observed to a height of 17 km (H_E). Data on the light curve, the radiation spectrum, and the dynamics of motion of the principal body and the fragments were analyzed in detail [10, 61]. Here we give briefly the basic data of observations and their analysis since this bolide is typical and is studied in greatest detail.

The mass of the Benešov meteoroid, which caused a bright radiation "burst," is estimated at 3-4 ton [10, 60, 61]. It was a rather large meteoroid, of the order of 1 m in radius. According to evaluations [62, 63] based on data of satellite observations [64, 65] that will be discussed below in greater detail, 20–60 such bodies (with an initial kinetic energy of 0.1–0.2 kton in TNT equivalent) arrive at the earth's atmosphere each year. According to the evaluations of [66, 67], the number of these bodies is about 300 a year. Apparently, the latter value is highly overestimated (see below).

The first breakup of the Benešov meteoroid occurred at dynamic pressures $\rho_a V^2$ of about 0.1–0.5 MPa (at heights of 55–60 km), and this comparatively low strength is consistent with data of observations of other meteoroids [9]. Owing to the low density of the atmosphere at great heights the fragments were retarded weakly and diverged with low velocities.

Lower, at a height of 30 km, five fragments following trajectories that differed from the main trajectory were seen. They were formed at heights of 37–39 km, where strong breakup accompanied by a bright burst of radiation occurred at a pressure of about 2.5–3.0 MPa. We note that this fragment motion could be recorded by

optical equipment only if the distance between them was larger than 20 m. Investigation of the stages of the breakup, formation, and expansion of a cloud of large and small fragments, dust, and vapor for any real event has never met with success up to the present.

The main burst of the Benešov meteor occurred at a height of about 24 km when the dynamic pressure attained 9 MPa. Below 23 km the main trajectory broke down into three individual trajectories. The bolide was seen to 17 km, but below 21 km the sensitivity of the equipment no longer permitted recording of the flight of individual fragments.

Dynamic Model of Fragmentation. The significant role of fragmentation in the process of meteoroid motion has been emphasized in many works (for example, [19, 68-73]). However the broken-up body can penetrate rather deep into the atmosphere. The concept of "inertial survival" was introduced for the first time by Grigoryan [74]: even if a body lacks strength, time is required for its mass to be accelerated in the direction lateral to the trajectory. Generally, the motion of the fragments formed is considered to be the travel of individual bodies diverging due to aerodynamic interaction [19, 70, 71, 75] or the expansion of one broken-up body in the liquid approximation [1, 76-78].

To analyze the process of breaking up itself, the Grady and Kipp model [83] was introduced [80-82] in the SALE hydrodynamic program [79]. It assumes that the defect distribution conforms to Weibull's statistical law [84, 85]. Fissures increase with load but, in this case, unloading in their vicinity occurs.

Calculations for an ice comet with a radius of 2 km entering the atmosphere of Jupiter with a velocity of 60 km/sec showed that breakup begins at a height of about 67 km. At the height $Z = 0$ where the air density is $\rho_a^0 = 0.17$ kg/m^3 and the pressure on the frontal surface is already about 6 GPa, the body is broken up completely.

In [86], the stresses in a meteoroid penetrating into the atmosphere were determined under the assumption that they can be expressed linearly in terms of strains, the latter being small, just like local velocities and shifts. The distribution of the pressure on the surface was prescribed from the solution of the corresponding aerodynamic problem. The instant when the volume of the broken-up region occupied 5% of the body's volume was taken conventionally as the beginning of the process of breaking up. Breakup of 30–40% of the volume was defined as the intermediate phase, while the stage where the breakup region covered approximately 55% of the volume of the body and reached its surface was referred to as the final phase. For stony monolithic meteoroids, a tensile strength of 20 MPa and a compressive strength of 200 MPa were used. But because of the multicomponent nature of meteoric bodies and their inhomogeneity and initial fissility the real strength even of strong meteoroids is much lower. In general, the adopted models fail to allow as yet for the original existence of large fissures that separate meteoroids into individual blocks.

For stony and iron meteorites, the strengths of their specimens are measured [87, 88]. It is of interest that the strengths even for pieces of one meteorite can differ by a factor of 2–3 and the limiting stresses themselves correlate weakly with the chemical-petrological composition of the meteorite. Thus, some iron meteorites turned out to be less strong than stony meteorites. On the average, the limiting tensile strength of the tested specimens σ_t ranges from 20 to 50 MPa while the compressive strength σ_c is approximately an order of magnitude higher. However the strength of inhomogeneous bodies is much lower than the strength of the homogeneous monolithic pieces that compose it. Thus, for a fragment of the Sikhote-Alin meteorite (of mass $m_s \sim 1$ kg), $\sigma_t = 44$ MPa, while the strength of single-crystal iron is an order of magnitude higher. The strength of large meteoroids or their fragments is lower than the strength of small specimens, on which experiments are usually carried out. Since meteoric bodies are inhomogeneous as far as the strength is concerned, the characteristic loads for which meteoric bodies of mass M break up in their motion in the atmosphere turn out to be lower than the strength limits of small specimens of a meteorite σ_s of mass $m_s \ll M$ [87]. Large defects are more rare than small ones, and the probability of their appearance increases with the volume of the body. On breakup the smaller fragments formed turn out to be stronger than the parent body. The variation of the strength of a meteoroid with its mass M can be evaluated by the relation

$$\sigma = \sigma_s \left(\frac{m_s}{M}\right)^{\alpha} = \sigma_s \varphi . \tag{6}$$

The quantity α is determined by the degree of homogeneity. The more homogeneous the body, the smaller is α. The same expression can be employed to determine the strength of a fragment σ_s of mass m_s if the strength of the parent body σ of larger mass M is known.

According to [89], a good estimate of α for meteoroids is $\alpha = 1/4$. With this exponent, the initial mass of the meteoroid $M = 10$ ton, and the mass of small fragments $m_s = 1$ kg the coefficient $\varphi = 10$. We note that if α is established on specimens of different dimensions in the range of 1–10 cm, extension of dependence (6) to bodies with a dimension of 1–100 m can cause significant errors. Therefore, in [90], it is proposed to introduce α as a function of the dimensions of the body and to gradually decrease the exponent as the dimensions increase. However, the law of change of α as a function of M remains to be established.

The distribution of the number of fragments formed on breakup N_m over masses m is unknown. In the calculations of progressive fragmentation described below, use was made of a distribution obtained in experiments on catastrophic impact breakup [91]:

$$\frac{dN_m}{dm} = Cm^{(k/3-2)}, \tag{7}$$

where the exponent is $k = 1.2$.

We note that the distribution of the fragments of the Mbale meteorite, shattered at a low altitude [92], obeys the indicated law. The velocity of entry of this body is estimated at 11–14 km/sec while the total mass is estimated at approximately 190 kg. On the earth, 150 kg of meteoric material was collected.

In [93], attention is drawn to a special feature of dynamic breakup. A sufficient condition consists in the presence of defects. However, the breakup energy needed for the objects to be broken down into two parts exists (it is one-two orders of magnitude larger than under conditions of statics). Accumulation of a certain store of elastic energy that ensures breakdown of the body is required. Since the latter is proportional to the cube of the size while the energy required for breaking down the fragments is proportional only to the square, the effective strength is inversely proportional to the size.

Dynamics of a Broken-up Bolide. The dynamics of the Benešov bolide was modeled under two assumptions – using a simple liquid model of the type of [34, 94] and the progressive-fragmentation model [75]. In both cases, the divergence of the fragments was considered to obey the simple law

$$u = kV\sqrt{\rho_a/\rho_0}\,. \tag{8}$$

This expression was employed earlier, in particular, in [19, 70]. The interaction of the shock waves of individual fragments was considered to lead to the appearance of a lateral velocity. An analysis of crater fields showed that k lies within 0.17–1.5 [19, 70]. Laboratory experiments for flow along two bodies (with comparatively small Mach numbers – of the order of 4) confirmed the fact of "repulsion" of the fragments [96]. Three-dimensional numerical calculations for two pieces in the form of semicylinders [97] showed that the aerodynamic interaction can be approximated by (8) with $k = 0.45$ if $d > 0.5R$. For larger distances, $k = 0$. In three-dimensional calculations [75] for a cubic body disintegrating into a large number of fragments (up to 27), $k = 0.44$ is obtained without allowance for evaporation.

The solution of the problem of interaction between fragments without allowance for evaporation has properties of similarity, i.e., the results obtained for one height are extented to any other size, any other dimension, and any velocity (if the effective adiabatic exponent as a function of temperature and density and hence velocity and height is disregarded). However, evaporation breaks the similarity. This issue was cleared up in [98] for the case of the motion of two chondrite bodies with an initial size $R = 1$ m at heights of 50 and 70 km in the earth's atmosphere with a velocity of 20 km/sec. Radiation transfer was calculated in a four-group approximation using tables of optical and thermodynamic properties of chondrite vapor [99].

With small distances d between the bodies ($d < 0.2R$), small vortices are formed in the evaporating liquid that increase and decrease the thickness of the vapor layer, disappear subsequently, and appear again. With large distances ($d > 0.3R$), a quasistationary regime of flow is established as rapidly as in the calculations without

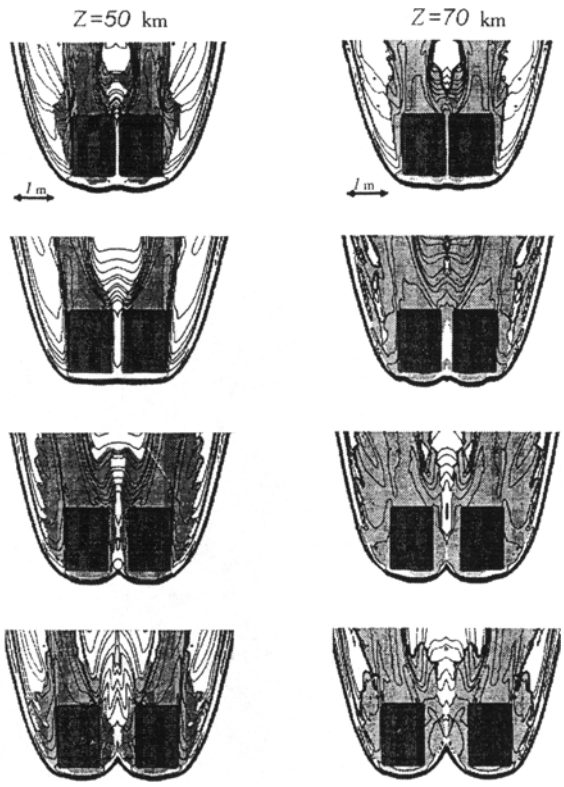

Fig. 1. Isolines of density for various distances between chondrite fragments at height of 50 and 70 km.

allowance for radiation. The coefficient of resistance is independent of the distance between the bodies. The lift coefficient, conversely, is maximum with small distances between the fragments and decreases rapidly as $d \approx R$. Here it differs slightly from the coefficient without evaporation, i.e., the vapor has no substantial effect on the mechanical interaction between the fragments. The heat-transfer coefficient is approximately twofold-threefold larger than for an intact body. The air is heated in the shock wave to a temperature of 1.2–1.4 eV and radiates intensely in the UV spectrum. The vapor absorbs the radiation, is heated, and reradiates in the visible and IR ranges. The vapor temperature attains 0.6–0.7 eV at the boundary with air and decreases to 0.2–0.3 eV near the body's surface.

Density fields obtained in calculations [98] with allowance for evaporation for two fragments are given in Fig. 1 for flight heights of 50 and 70 km and different distances between the bodies. The vapor is shown in gray. It can clearly be seen how, inside one shock wave of intricate shape, the bodies move, each in its own vapor cloud. The instabilities that develop at the boundary of the vapor cloud and the interaction between the shock waves lead to strong turbulization of the gas. This effect manifests itself more strongly for a large number of bodies and, accordingly, intersecting shock waves (calculations for 13 fragments are also given in [98]).

In [75, 97], the fragments were assumed to have identical mass. A strong difference in the masses of the fragments also leads to a substantial increase in the divergence velocity for small fragments, namely, by a factor of 3–7 if the mass of the small fragment amounts to 2–10% of the mass of the main body. Laboratory experiments [100] showed that, in addition to repulsion, we observe the opposite effect – collimation, i.e., formation of a narrow jet of small fragments moving in the trail of the leading, largest fragment. This effect was also confirmed by calculations [75].

Comparison of the angles at which the fragments of the Benešov meteoroid diverge, calculated by (8), with the angles obtained in observations shows that at a height of about 30 km there is agreement for some fragments as far as the order of magnitude is concerned; for others, the disagreement attains a factor of 4–6 [10]. We assume that this is due to the strong difference in masses and the intricate shape of the fragments. At a height of 25 m, the fragments diverge at an angle of about 0.3°, which is in agreement with the evaluation by (8). Thus, the opening of the jet of the fragments is small, and they interact aerodynamically for a rather long time [75]. By the time of

intense fragmentation at a height of 25 km accompanied by a bright burst, the velocity along the trajectory is about 18 km/sec and the total mass of the fragments is estimated at approximately 1000 kg. Consequently, at the given height, the decrease in the mass as compared to the initial mass is very pronounced now for the meteoroid under consideration. Upon fragmentation the velocity of fragment motion along the trajectory is only 6–9 km/sec and the dynamic masses are of the order of 0.4–3 kg (with a density of 3.7 ton/m^3). As is evident, deep-penetrating fragments have a mass that is 3 orders of magnitude smaller than the initial mass. Some fragments with a mass of 2–3 kg attained a height of 18–20 km with a velocity of 5.1–5.3 km/sec and then moved while invisible to observers. Some of the fragments could reach the earth.

The three-dimensional configuration of the fragments observed for Benešov at various instants agrees with the configuration in calculations [10]. However, the details of the fragments' flight can hardly be reproduced theoretically, much less be determined beforehand. They can be predicted only statistically since the process of breaking up itself and the number and shape of the fragments depend significantly on the history of the meteoroid prior to its entry into the atmosphere [101].

Breakup of a "Liquid Drop." For large meteoroids penetrating rather deep into the atmosphere without substantial retardation, the pressure on the surface is so much larger than the strength that, to describe the breakups and expansions of the cloud of fragments, we can adopt the liquid model, which fails to allow for the strength from the outset of entry into the atmosphere. In considering the motion of a strongly broken-up body in the form of a "liquid drop," i.e., a body devoid of strength, by two-dimensional calculations [1, 78] it was found that under the action of aerodynamic forces the body becomes highly strained with a "breakthrough" being formed along the axis, i.e., in the zone of the maximum load. Because of the development of Rayleigh–Taylor and Kelvin–Helmholtz instabilities the body is separated into regions with a significantly differing density, which can also be considered to be fragmentation.

For an originally spherical ice body of radius 100 m with an initial velocity of vertical entry of 50 km/sec, pronounced loss of stability was observed even at a height of 25 km, breakthrough along the axis occurred at heights of 4–5 km, and at a height of 2.5 km above the surface the body increased its diameter by a factor of 1.5. The length of the fragmenting body also increased by a factor of 1.5, i.e., the average density decreased by approximately a factor of 3. The most dense pieces of material ("fragments") contained 80% of the initial mass and more than 70% of the initial energy. With a larger radius ($R \sim 200$ m) the meteoroid, reaching the earth's surface, was still unbroken. Unfortunately, analogous calculations, because of their cumbersome nature, have yet to be made for bodies of smaller radius, say, 30–50 m, i.e., about the radius of the Tunguska meteoroid. We note that in two-dimensional calculations [82] the rate of expansion of the broken-up body turned out to correspond to (8) but for $k = 2$.

Numerical calculations of the motion, in the atmosphere, of a body when its surface is highly strained necessitate the development of special methods. The Lagrangian approach used, for example, in [78, 102] is often hindered by rapid deformation of the grid, which requires frequent reinterpolation. In the case of the Eulerian approach, we need to use explicit separation of the contact boundary. In [78, 103-105], a technique based on an algorithm similar to the VoF (Volume of Fluid) method [107] was employed. Normalization of the volumes occupied by different media in combined cells enables us to determine more accurately the position of the contact surface in these cells. This permits consideration of not only singly connected regions but also multiply connected regions, for example, in the process of fragmentation of the body. We note that subsequently similar problems were solved in [108-111] using the SOVA procedure [112], which is analogous to the CTH method [113] in many respects.

Apart from ordinary testing of difference schemes and programs that realize them the problem of the adequacy of the employed models for the real processes in entry of a meteoroid into the atmosphere arises, in particular, the correctness in describing the loss of stability by the boundary of the cloud of vapor and its mixing with air. In this connection, we note the testing of a free Lagrangian scheme [78, 102] by comparison of calculation results with a laboratory experiment on asymmetric laser explosion [114, 115] and with data of experiments on retardation, in air, of a high-speed jet of explosive generators with energies of the order of 10 MJ and velocities up to 60 km/sec [116]. The SOVA procedure was also tested in this kind of experiments [117]. In general, retardation of a weakly diverging high-speed jet in air is a rather close analog of retardation of a vapor cloud around

a meteoroid that evaporates intensely while moving through the air, including radiation transfer, since the velocities and hence the temperatures as well as the densities of the vapor and the air and the characteristic dimensions and hence the optical thicknesses are rather close to those for real meteoroids [117].

Analytical Evaluation of Retardation and Expansion of Meteoroids without Strength. There are several approximate analytical models [19, 34, 56, 70, 74, 94] that differ slightly (see, for example, [73] for a discussion of these differences). However, the results of their use as a first approximation are described by expression (8). Let us obtain another simple approximate model. Assuming conservation of the mass and shape of the originally spherical drop of liquid, i.e.,

$$\rho_0 R^3 = \rho_0^0 R_0^3, \tag{9}$$

and that the atmosphere is exponential, i.e.,

$$\rho_a = \rho_a^0 \exp\left(-\frac{Z}{H}\right), \tag{10}$$

using (1), (2), and (8), we can obtain a simple analytical solution for the radius R of the body:

$$R = R_0\left[1 - \left(\frac{kH}{\sin\theta}\sqrt{\left(\frac{\rho_a}{\rho_0^0}\right)\frac{1}{R_0}}\right)\right]^{-2}. \tag{11}$$

From (11) the similarity law follows – the height at which the same degree of breakup is attained ($R/T_0 = \text{const}$) is identical for bodies for which

$$\frac{\rho_a}{\rho_0^0 \sin^2\theta}\left(\frac{H}{R_0}\right)^2 = \text{const}. \tag{12}$$

is fulfilled. The applicability domain of this criterion is much wider than that of the model (11) itself. It enables us to convert results of detailed calculations or experimental data for bodies of different densities ρ_0^0 and different radii R_0 that enter the atmosphere at different slopes θ of the trajectory to the horizon to other values of these parameters. It is significant that the velocity of the body is not involved in (11) and (12).

The loss of stability depends on the shape of the body, while this shape itself changes in the process of deformation. The characteristic height H is not constant. Finally, transfer of thermal radiation and ablation do play a certain role. Therefore the similarity indicated can be used only for approximate estimates. Furthermore, calculations [111, 118] showed that the internal structure of the body (the distribution of inhomogeneites in it) also governs substantially the depth of its penetration into the atmosphere (when the average densities are identical, bodies with dense disseminations penetrate deeper). On the one hand, this means that we must resort to numerical computational methods that allow for structural inhomogeneity. On the other, their results should be understood only in the statistical sense, and therefore the calculations themselves must be multivariant.

"Sand Bag" Models. To describe the process of expansion of the cloud of fragments and vapor, one employs not only quasiliquid models but also "sand bag"-type models [78, 105, 119]. An advantage of the latter is that they allow for the evaporation of the fragments in the cloud, which is faster, the more numerous and the smaller they are. At the same time, in quasiliquid models, allowance is made only for evaporation on the cloud surface. In describing the behavior of small "sand grains" in air, the momentum change due to evaporation and energy losses by evaporation were allowed for.

In [1, 119], consideration was given to penetration, with a velocity of 20 km/sec, of a great many, namely, 10^6, fragments that originally filled the volume of a body 100 m in radius. The fragments were separated into five groups with a size of 0.1 to 10 m and an average size of 1 m (in this case, we are dealing with "rubbles" and "piles" rather than "sand grains"). Calculations without allowance for evaporation [1, 119] showed that a meteoroid reaches a height of 7.7 km in the form of a weakly expanded cloud with a radius of approximately 120 m while it reaches the earth in the form of a cloud with a radius of approximately 200–250 m, its extent along the trajectory being

about 350–400 m. A laminar structure of the cloud associated with dissimilar retardations of fragments of different sizes is detected.

The increase in the volume of a body as its average density decreases leads to attenuation of the impact force [120] and increases the fraction of the energy that becomes kinetic and thermal energies of a vapor jet gushing upward but does not eliminate the process of crater formation in the hard earth or formation of an unstable crater in water.

In [121], allowance is made for the interaction of a compact "swarm" of particles with the plasma flux. In an improved "sand bag" model [122], the change in the particle size in successive fragmentation due to both the growing aerodynamic load and collisions between fragments is taken into account.

The mechanism of repulsion of the fragments due to their collisions in the case where the number of fragments exceeds a critical value is also introduced in [122]. This prevents the fragments from accumulating in small regions.

As we have already noted by the example of the Benešov meteoroid, the process of the body's fragmentation frequently occurs more than once. After a certain time, large fragments leave the retarded cloud of vapor and small fragments and move individually. This should be allowed for in future theoretical models that must be a combination of the methods of the type of [34, 75, 95] with the type of [78, 119].

These models must be processed with allowance for observation data. Let us describe them further; we will use not only dynamic data but light curves as well.

Radiation Efficiency. Catalogs of bolides of the Prairic Network [123-125] give the photometric mass M_{ph} obtained in meteoritics by a method [126] that is based on experimental data on small (gram) artificial meteoroids [127]. The corresponding radiation efficiency η, i.e., the ratio between the energy of a luminous-radiation pulse and the initial kinetic energy, amounts to only 0.01–0.1% [126]. This approach to large bolides is criticized in [63]. The criticism is based on the fact that an increase in the dimensions of the body with the same velocity of motion and flying height increases the optical thickness, altering the radiation spectrum, which changes progressively from the line spectrum of a volumetric radiator mainly due to atomic and ionic lines and molecular bands of the vapor to the spectrum of an optically thick shock-compressed layer of air [128-130]. The efficiency of conversion to radiation also changes accordingly [25, 62], attaining, in the limit, values that are close to those for a powerful explosion [131].

Systematic calculations of the radiation efficiency, the radiation spectrum, and the ablation velocity for bodies of different dimensions were performed according to the model of [132]. Use was made of the analogy between the one-dimensional cylindrically symmetric unsteady motion of a gas in piston travel and quasistationary hypersonic flow [133, 134]. It was taken into account that under the action of intense radiation from the shock-compressed air layer on the piston (or the body) a vapor layer occurs that is heated and begins to radiate itself [25]. The spectrum and fluxes of the radiation were determined by solution of the transport equation with a very large number of spectral intervals (about 15,000) in both the air and the vapor, detailed tables of optical properties of the hot air [135] and the vapor [99] being used. The composition of the vapor of meteoroids of various types was taken in accordance with [136], and for comets – according to [137]. An important role in the spectrum of meteoroids, not just iron ones, is played by numerous iron lines (1717 FeI lines were allowed for in the tables of [99]) and molecular bands of oxides of iron and a number of other elements.

We note that comparison [61] of calculated spectra [132] obtained with the use of the tables of [99] and spectra recorded in entry of the Benešov meteoroid [60] showed that their general form at different heights coincides. All the predicted lines are detected in observations. The characteristic emission temperature of atomic lines is 5000–6000 K in both calculations and observations. The role of the continuum increases while the role of the lines decreases as the flying height decreases [61]. However the isolated disagreements noted in [61] point to the need for improvement of the computational model of radiation.

The ablating-piston model has both drawbacks and advantages. Among the drawbacks are use of the assumption that the axial velocities of the vapor and the air are identical and are equal to the velocity of the body and the fact that turbulence and mixing at the vapor-air interface and in the vapor itself are not allowed for. In the model of [123], breakup of the body is not allowed for. When the results of [123] are used to describe real

events [10, 61, 95] fragmentation of the body is considered, for example, as occurring in accordance with (6) under the assumption of expansion of the cloud of vapor and fragments by relation (8). Therefore in what follows, it is appropriate to make two-dimensional and three-dimensional unsteady radiation-gasdynamic calculations and to refine the emittances. Among the advantages of the ablating-piston method is its comparative simplicity, which permitted calculation of a great many variants for meteoroids of different dimensions and compositions that move with different velocities at different heights.

Comparison of results of calculating the radiation intensity with data of observations for a known flying height and velocity enables us to determine the instantaneous radius of the body [131], i.e., the effective radius of the body that will yield the same radiation intensity as the intensity observed. A sharp increase in the radiation radius in the period of "burst" indicates intense fragmentation and rapid expansion of the cloud of fragments and vapor. The radiation radius apparently depends on the composition of the body, while the corresponding radiation mass calculated at heights above the first intense burst depends in addition on the assumptions about the shape of the body and its density. This brings about an uncertainty in the evaluation of the "radiation" mass. Incidentally, the same is true for the dynamic mass determined from the body's retardation in the atmosphere. A combination of both approaches improves the reliability of evaluations.

Specifying a model of retardation of the body, its breakup, and expansion of the cloud of fragments, we can find the radiation pulse for a prescribed initial mass and velocity of the body and determine the integral radiation efficiency η_i, i.e., the ratio of the total radiation energy to the initial kinetic energy. The results of calculations [64] were approximated by the following expressions:

$$\eta_i = 0.021 \log E_r + 0.0031V + 0.037 \text{ (for iron meteoroids)},$$

$$\eta_i = 0.021 \log E_r + 0.0055V + 0.022 \text{ (for N-chondrites)}, \quad (13)$$

where the velocity V is in km/sec and the radiation energy E_r is in kton in TNT equivalent. If the velocity of the body is unknown, it is appropriate to employ the averaged curve

$$\eta_i = 0.021 \log E_r + 0.103 \text{ (for N-chondrites)}. \quad (14)$$

We note that η_i depends not only on the chemical composition of the meteoroid but also on the spectral sensitivity of the device. The coefficients in (13) and (14) are given for photoelectric detectors with a transparency window of 1–3 eV [65] and a sensitivity maximum that corresponds to the maximum of blackbody radiation at a temperature of 6000 K [28]. For the panchromatic photographic films used in ground observation networks, η_i is approximately a factor of 1.5 lower [138].

Calculations of the integral radiation efficiency η_i (in the entire flight time) showed that this quantity increases with the size of the body moving in the atmosphere and with the corresponding optical thickness. For bodies with dimensions up to 10 m at heights greater than 20 km, the radiation spectrum is still far from the spectrum for an optically opaque plasma and is governed to a large extent by the lines and molecular bands of the vapor. Only for very large bodies (of ~100 m or more) is the radiation governed mainly by shock-compressed air [128-130], and heat transfer in the vapor is radiant heat conduction in character.

Thus, for bodies with a mass of the order of 100 kg and a kinetic energy E_k of the order of 5–10 tons in TNT equivalent, the calculated radiation efficiency η_i is an average of about 2–4%. This is in agreement with empirical data on Lost City, namely, 45% with a velocity of 20 km/sec, 1.8% with 10 km/sec, and 0.5% with 5 km/sec [11]. For bodies with a mass of 10–100 tons and an energy E_k of the order of 0.5–5 kton in TNT equivalent, we obtain η_i of about 8–10%. These values are much lower than the values for nuclear explosions, namely, ~30% [28]. This is associated with the progressive character of energy release and with a significantly different shape of the radiating region – extended, stretched strongly along the trajectory rather than spherically symmetric.

Prairic Network Bolides. Data on 334 bright bolides were published in catalogs [123-125]. Bright (the magnitude is $m < -8^{mag}$) and slow ($t > 2$ sec) bolides were selected out of a total number of 2700 meteors. Among

TABLE 1. Parameters of PN Bolides That Penetrated into the Atmosphere below 30 km

PN (No. in catalog)	m_{max}	M_{ph}, kg	V_B, km/sec	H_B, km	H_{max}, km	H_E, km	Z_R, deg	V_E, km/sec
38651	VB	–	13.8	77.1	–	16.4	52	–
38768*	−13.0	160	17.7	70.4	53.6	29.3	38	8.8
39113A	−11.1	34	15.0	72.4	33.7	26.5	23	8.0
39182	−9.6	4.45	17.6	78.3	35.2	28.0	33	7.1
39240	−11.1	29.5	17.1	78.0	29.3	22.7	30	6.1
39404	−10.7	19.5	15.4	79.2	46.5	28.2	34	4.5
39406A	−15.7	260	17.2	68.0	32.5	29.7	39	10.2
39434	−14.2	2150	14.6	77.0	32.3	26.9	60	6.9
39470*	−18.0	8500	23.6	79.2	33.3	22.2	56	9.3
39512*	−12.0	40.5	20.2	81.7	35.8	27.8	45	13.1
39815	−9.3	20.5	13.3	76.4	46.2	27.0	52	4.0
39863A	−9.2	3.95	20.5	76.6	39.8	28.9	35	7.1
39921C*	−10.8	55	14.5	67.7	31.9	24.9	15	7.6
39935	−10.9	55	17.9	83.9	36.3	22.0	33	7.4
40151A	−11.2	170	13.4	67.5	31.8	23.3	50	5.2
40301A	−8.2	3.7	15.8	74.2	44.5	29.4(31.6)	44	8.9*
40428B	−8.1	3.15	15.5	79.1	49.3	29.7	45	6.9
40503	−20.0	17,500	21.0	92.7	23.4	21.3	52	11.7
40590	−11.6	245	14.2	85.9	31.7	19.5	52	3.4
40617	−9.1	39	13.2	78.9	35.5	26.6	59	4.6
40660B	−9.8	4.1	26.5	92.9	48.7	28.8	54	6.1
40806	−8.6	12.5	13.3	82.1	38.8	29.3	56	5.7
40910*	−8.8	11.5	16.9	78.8	52.8	26.3	49	6.8
40996	−7.5	5.5	13.7	71.5	51.7	25.3	54	4.2
41132*	−10.6	23.5	16.8	82.2	46.8	19.4(35.8)	42	16.1*
41275*	−10.0	55	13.1	78.7	31.0	19.6	43	3.8
41298	−9.8	16	15.2	75.9	43.1	28.8	28	6.9
41844	−9.9	9.5	16.0	77.2	39.6	28.0(31.7)	33	10.7*
42121	VB	–	16.3	74.9	–	29.5	50	–

Notes: VB is very bright; *, denotes that the velocities were determined at heights larger than H_E (they are indicated additionally in the parentheses of the H_E column). The brightness of the fireballs marked by asterisks in the first column was estimated less accurately than the brightness of the second group of fireballs [124].

Fig. 2. Peekskill bolide.

them, only 31 bolides had a final height of under 30 km, 9 of them reached 25 km, and only 4 reached a height of 20 km. Although some fragments could penetrate deeper, down to the earth, in the next, dark stage of flight it is apparent that a major portion of the energy is released at heights of 20–30 km or more. For 29 of the deep-penetrating bolides, the so-called corrected photometric masses obtained upon analyzing the data for Lost City and Innisfree [139, 140] are given in Table 1. It became clear that the η employed traditionally are highly understated. For these bodies, the radiation efficiency η_i turned out to be of the order of 1–2%. After this the photometric masses in [141, 142] were decreased twofold as compared to the photometric masses given in catalogs [123, 124].

TABLE 2. Some Parameters of Deep-Penetrating PN Bolides

PN (No. in catalog)	M_{ph}, kg	M_B, kg	M_r, kg	H_E, km	V_E, km/sec	Type of bolide	Breakups		M_E, kg
							dynamic [141, 142]	radiation [138]	
39113A	34	98	14	26.5	8.0	II	NF	U	3.6
39240	29.5	20	11	22.7	6.1	I	NF	U	7.0
39404	19.5	2.8	13	28.2	4.5	I	1F	Y	0.3
39406A	260	92	32–66	29.7	10.2	II	MF	Y	6.0
39434	2150	3600*–850	720	26.9	6.9	I	NF–MF	Y	1080
39935	55	28	10	22.0	7.4	I	NF–MF	U	–
40151A	170	42	29–63	23.3	5.2	I	MF	Y	–
40503	17500	1910*–560	600–750 560	21.3	11.7	II	NF	Y	350
40590	245	163	120–150	19.5	3.4	I	2F	Y	16

Notes: Classification according to the gross-fragmentation model: NF, no breakup; 1F, one breakup; MF, many breakups; classification according to the radiation radius: U, not determined; Y, breakup; *, with a density of 2 g/cm^3.

TABLE 3. Data for Bodies Penetrating below 25 km

PN (No in catalog)	m_{max}	M_{ph}, kg	V_B, km/sec	V_{30}, km/sec	V_{25}, km/sec	V_{30}/V_B	V_E, km/sec	H_E, km	M_B, kg	M_r, kg
39240	–11.1	29.5	17.1	13.1	9.6 (25.5)	0.77	6.1	22.7	20–16	11
39470*	–18.0	8500	23.6	22.5 (32.7)	19.9 (26.7)	0.95	9.3	22.2	–	1300
39921C	–10.8	55	14.5	11.7 (32)	7.6	0.81	7.6	24.9	–	24
39935	–10.9	55	17.9	14.2	11	0.79	7.4	22.0	28	10
40151A	–11.2	170	13.4	9.8 (29.9)	7.8 (26.2)	0.73	5.2	23.3	33–42	29–63
40503	–20.0	17500	21.0	18	16.5 (27.1)	0.86	11.7	21.3	1910*–560	600–750
40590	–11.6	245	14.2	11.6	8.4	0.82	3.4	19.5	163	120–150
41132*	–10.6	23.5	16.8	16.1 (35.8)	–	0.96	–	19.4	–	–
41275*	–10.0	55	13.1	12.3 (33.7)	10.4 (27.5)	0.94	3.8	19.6	–	32

Note. In the parentheses are values of H; V_{25} and V_{30} are the velocities at the corresponding heights.

Analysis of the Prairic Network bolides [9, 138] showed that the meteoroids that caused them break up at a pressure of 0.1–1 MPa, i.e., at heights of 70–35 km (depending on the velocity of entry, the slope of the trajectory, and the type of meteoroid). According to a videotape of the Peekskill bolide [143], it broke up intensely at a height of about 41 km at pressures in the interval of 0.7–1 MPa. Up to 70 fragments were recorded. Figure 2 gives a typical photograph. We note that at least one of the smallest fragments reached the earth and was detected.

Photometric data on the brightest bolides have been analyzed again recently [141, 142]. To investigate 48 bolides brighter than -10^{mag} with "good" photometric data, use was made of the "gross fragmentation" model [9]. The corresponding more accurate initial velocities, heights of the beginning (H_B) and end (H_E) of the visible trajectory, and maximum-brightness heights H_{max} as well as the initial (M_B) and final (M_E) dynamic masses are given in Tables 1 and 2. The radiation masses [138] are also given in Table 2, where the types of fragmentation

TABLE 4. Largest Bolides Recorded by the European Network

Event	Date	Name	m_{max}	Preatmospheric mass, kg	Type of bolide	H_B, km	H_{max}, km	H_E, km	V_B, km/sec
19241	07.04.1959	Přibram	−19.2	11000	I	98	46	13	20.89
EN151068	15.10.1968	Cechtice	−15.5	800	II	72	45	30	19.02
EN100469	10.04.1969	Otterskirchen	−15.4	2500	II	84	45	24	16.08
EN241170	24.11.1970	Mt.Riffler	−15.1	1500	I	83	41	26	21.17
EN170171	17.01.1971	Wirzburg	−17.0	3200	IIIb/II	75	60	45	15.7
EN041274	04.12.1974	Šumava	−21.5	3000	IIIb	99	73	55	27.0
EN010677	01.06.1977	Freising	−16.9	2600	II	78	47	27	27.0
EN140977A	14.09.1977	Brno	−16.2	1500	II	97.8	60	40	30.2
EN070591	07.05.1991	Benešov	−19.5	7500	I or II	98	26	16	21.1
EN220293	22.02.1993	Meuse	−17.3	3000	I	77	–	21.5	26.7
EN221095	22.10.1995	Visla	−17.1	900	IIIb	–	–	–	–
EN251095A	25.10.1995	Tisza	−16.1	890	I	80.5	–	26.5	29.22
EN231195	23.11.1995	J.Hradec	−16.9	3600	I	93	–	20.4	22.197

determined by the model of [9] and the evaluation of whether breakup occurred by the model of [138] are also indicated. All these bodies are referred [141] to type I or II, i.e., to stony bodies or carbonaceous chondrites with a density of 3.7 to 2 ton/m^3. Both models yield that most of these bodies broke up in the atmosphere at pressures of 0.4–4 MPa although some of them remained intact even at maximum pressures of 6 MPa. Thus, the strength of meteoroids even from one group varies within rather wide limits.

The final mass M_E of all the indicated meteoroids did not exceed several kilograms, except for PN 39434 and PN 40503. It should be noted that for PN 40590 accompanied by the fallout of the renowned Lost City meteorite, the initial velocity was low, namely, 14.2 km/sec. It fragmentated at heights of 40, 30, and 23 km at pressures of 0.1, 0.5, and 3 MPa. A great many fragments were seen at heights of 30–25 km. The initial mass was estimated at 160 kg, and a meteorite with a mass of 17 kg was found on the earth.

Only 9 out of 331 bolides (3%) were detected below 25 km. Data for them are given in Table 3. All of them are brighter (-10^{mag}), up to -20^{mag}. This is due to the fact that very bright bolides are rare while less bright meteors are caused by smaller bodies that either evaporated totally or were retarded so that the temperature decreased to very low values, and they became invisible.

Table 3 includes the masses determined both by the dynamic method and from the radiation radius. These values are not in contradiction with each other but, for the brightest bolides both are much lower than the photometric masses of even the "corrected" scale. This is due to the fact that, for larger bodies, the radiation efficiency is actually higher than is taken for the "corrected" scale [141, 142], and therefore the photometric mass is overstated [163, 138].

For comparatively small bolides (M_{ph} = 10–30 kg), there are no objections against employment of the corrected photometric mass if sufficiently convincing data on the dynamic or radiation mass are absent. We note that for these bodies, for example, for PN 39921C, 41275, 39240, and 39925, the photometric mass differs from the radiation mass by no more than a factor of 1.5–2.

The velocities at a height of 30 km turn out to be 1.05–1.36 times lower than the initial velocities, which is in reasonable agreement with the evaluations by (4) based on the relation between the specific mass of the meteoroid m_0 and the specific atmospheric mass m_a above 30 km.

Data for bright (brighter than -15^{mag}) bolides of the European Network with $M_{ph} > 1000$ kg were selected from [3-5] and are given in Table 4. We note that, according to [66, 67], about 3000 stony bodies with a mass of more than 10 kg penetrate into the earth's atmosphere every year. According to the evaluation of [144], approximately 15–25% of them penetrate to a height lower than 30 km, i.e., 500–800 bodies a year [66].

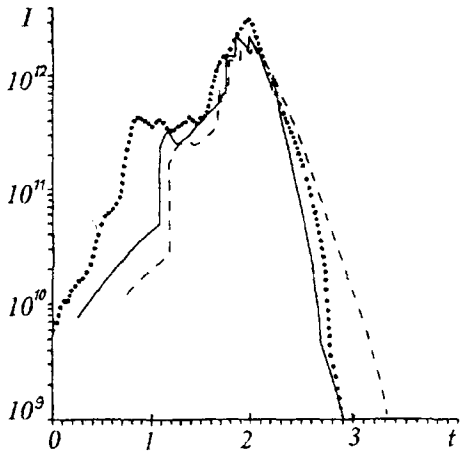

Fig. 3. Light curve of the event of February 1, 1994 (I, W/ster, points) and model light curves obtained using the progressive-fragmentation model for a meteoroid with an initial velocity V_0 = 25 km/sec and a mass of 500 tons under the assumption that it was iron (α = 0.25–16, σ_1 = 400 Mdyn/cm^2, solid curve) or chondrite (α = 0.3, σ_1 = 300 Mdyn/cm^2, dashed curve) vs. time t, sec.

Satellite Network (SN) Observations. The European Ground Observation Network covers only 0.3% of the earth's surface. In recent years, a global system that covers the entire earth has been added to a number of observation networks. It is several geostationary satellites equipped with photometric sensors with good time resolution [65].

SN data obtained on the magnitude and shape of a radiation pulse in the visible wavelength range were employed to determine E_k of meteoroids penetrating into the earth's atmosphere [62, 63] (in the E_k range of 0.06 to 40 kton in TNT equivalent). Results of systematic (22 months) satellite observations (51 events in 1994-1996) are analyzed in [63]. In the range of initial kinetic energies of 0.3–10 kton in TNT equivalent, the number of falls with an energy higher than E_k on the entire earth in a year is described well by the approximate expression

$$N = 10E_k^{-0.87}. \tag{15}$$

This expression (a "better estimate") was obtained earlier by Shoemaker in [30] based on data on lunar craters, the number of large craters on the earth, and the number of small meteoroids that penetrate into the earth's atmosphere.

According to results of acoustic observations carried out for 17 years [145], the approximation dependence of the number of falls on the energy is as follows:

$$N = 7.2E_k^{-0.7}. \tag{16}$$

The acoustic system in these years was local (on the territory of the USA) rather than global. A total of 9 falls of meteoroids were recorded. The probability of falls on the entire surface of the earth was determined by extrapolation. Relations (15) and (16) in the energy range of 7–30 kton in TNT equivalent agree well (the difference in the number N is no larger than 2). However the acoustic system recorded one fall with an energy of the order of 1 Mton in TNT equivalent and this apparently is the reason for the difference of the exponent in (16) from the exponent in (15). According to (16), one event with an energy of 1 Mton must be observed approximate;y every 20 years. Such powerful impacts have not been witnessed yet by the satellite system.

One of the largest events recorded by optical and IR sensors of the satellite system was the event of February 1, 1994 [146] with a meteoroid energy of about 30–40 kton in TNT equivalent [63, 95]. For this Pacific bolide (the entry into the atmosphere was recorded in the area of the Marshall Islands), one was able to determine the slope of the trajectory (~45°) and the initial velocity (24 km/sec) with the use of data from several geostationary satellites [146].

The light curve of this event is given in Fig. 3 (the points). A characteristic feature of it is the presence of two radiation peaks due to two main stages of breaking up. The fragmentation led to the formation of two clouds of fragments at heights of 34 and 21 km [146]. The same figure gives curves calculated by the progressive-fragmentation model for a meteoroid with a mass of 500 ton under the assumption that it was iron ($\alpha = 0.25-0.16$) with a strength $\sigma_t = 40$ MPa. Calculations showed that fragments reach a height of 16 km with a mass of less than 200 kg. The luminosity curve for a chondrite body with $\alpha = 0.30$ and $\sigma_t = 30$ MPa is given in the same figure.

In both cases, use was made of self-consistent ablation and luminosity coefficients obtained by the ablating-piston model [132]. As can be seen, it is difficult to prefer one or another variant of the composition of the body: for such a large body, the luminosities are quite similar owing to the large optical thickness of the shock-compressed layer of air and vapor. As far as the strength is concerned, breakup apparently begins at a pressure lower than the pressure taken in the calculations.

Based on the radiation energy and the velocity of the Pacific bolide, the mass of the meteoroid that caused it was about 300–500 tons [63, 95]. It is of interest to note that, according to [95], the mass of the Sikhote-Alin iron meteoroid of February 12, 1947 was approximately the same [147-149]. This event was analyzed again in detail recently [95] with the use of data of eyewitnesses on the trajectory, the glow intensity, and, above all, the distribution of numerous craters in the crater field: 27 of them with a diameter larger than 7 m were located on a 0.1×0.2 km area while a host of smaller craters covered an area larger than 1×1 km [150]. The largest crater had a diameter of 27 m, which corresponded [95] to the impact of the largest fragment with a mass of approximately 10 tons. According to [95], only 100–200 tons, or about 30% of the initial mass, reached the earth (and only 27 tons was collected [69, 147-150]). The kinetic energy of the fragments that reached the earth was 100 tons in TNT equivalent, which is an insignificant portion of the initial energy ($\sim 1\%$) and indicates clearly the shielding properties of the atmosphere, which, unfortunately, have a limit. The mass of the Sikhote-Alin meteoroid is nearly the same as for the Pacific meteoroid [95]. However, a smaller (by approximately a factor of two) velocity of entry leads to breakup at a lower height (at about 22–28 km originally, and then at heights of 10–16 km). Therefore rather large fragments of it penetrated down to the earth (with velocities of 1–2.5 km/sec). The first strong fragmentation of the Pacific meteoroid occurred at a height of about 50 km, and the second at a height of about 25–28 km. However, it is not improbable that fragments reached the ocean's surface (there were no eyewitnesses in the area of fall; the height of the clouds was 18–20 km).

According to (16), an event with such a high energy must be observed every two years. But in the time since 1994, falls as large is this have not occurred. This possibly suggests that for bodies with a kinetic energy higher than 10 kton in TNT equivalent the frequency of falls is lower than by (16), and relation (15) is preferable. Furthermore, a wavy character of the size distribution in the asteroid belt, i.e., a deviation from a simple power low, was predicted in a number of works on the theory of collisions and fragmentation of space bodies [151, 152]. However, it is possible that here there are simply significant fluctuations of the flow of large meteoroids, and averaging is acceptable only for a large number of years.

For some cases of satellite-based observations, it turned out to be possible to determine the height of the maximum intensity or the position of the remains of a meteoroid illuminated by the sun; these data are given in Table 5. As can be seen these heights are mainly 30–39 km.

In recent times, reports of systematic satellite observations have, unfortunately, stopped. According to data for some events that nonetheless were published, we made estimates of the energy of meteoroids, and they are also included in Table 5. Among these events is bolide SN 94166, for which the St. Robert meteorite was found [153]. This is the fifth meteoroid recorded in flight whose fragments were detected on the earth. With the initial energy determined from the integral radiation luminosity at 0.06 kton in TNT equivalent and an estimated velocity of entry of 13 km/sec the meteoroid mass was estimated at 100 kg. According to an isotopic analysis of the meteorite, the estimate of the preatmospheric mass was 0.7–4 ton, which is in agreement with the initial mass given above. The mass determined from the acoustic signal is given in [153] with a substantially larger spread, namely, 1–10 tons.

Furthermore, Table 5 includes the bright daytime bolide SN 97282 (El Paso) observed by thousands of eyewitnesses [154] and recorded by the US acoustic system and, finally, the Greenland bolide (SN 97343) [155]

TABLE 5. Estimation of Parameters of SN Bolides

Event and date	E_r, kg	I_{max}, W/ster	H_{max}, km	E_k, kton	M_0, ton	V_B, km/sec	η, %	η_i, %	Possible composition
88106 15 April 1988 90274	1.70	$1.4\cdot10^{12}$	43	8–9	25–45	48–50	18-21	11	Stone
1 October 1990 91277	0.57	$3.5\cdot10^{11}$	30	3–6	70–200	15–20	11–19	9.7	Stone
4 October 1991 94032	0.14	$6.6\cdot10^{10}$	33	0.9	20	15–20	15	8.4	Stone Iron
1 February 1994 94149	4.39	$3.2\cdot10^{12}$	34, 21	31	400	24[a]	14	12.5	Stone
29 May 1994 94307[b]	0.090	$9.9\cdot10^{10}$	34	0.6–2.5	2–140	< 50	3.5–15	8.0	–
3 November 1994 94350	0.56	$3.4\cdot10^{11}$	34[b]	3–5	70–200	15–20	11–19	9.7	Stone
16 December 1994 94166	0.0086	$2.8\cdot10^{10}$	30	0.07–0.3	0.25–17	< 40	3.3–4 17	5.9	–
15 June 1994 97282	0.0031	$4.0\cdot10^{9}$	36.2	0.063	3	13[a]	–	4.93	Stone
9 October 1997 97343	0.045	10^{11}	28–30*	0.6	–	–	–	7.5	–
9 December 1997	0.064	$9.5\cdot10^{10}$	40,28 –25	0.8	8	29**	–	7.8	–

Notes: [a]The velocity of entry is known from observations; [b] conversion by similarity from bolide SN 90274 based on E_r, I_{max}, and the form of the light curve; * according to data of acoustic measurements [154]; ** preliminary evaluation [155].

that provoked special interest since it fell in the polar region during the polar night and brightly illumunated a vast area. In spite of the small population of Greenland, it was also witnessed (mainly by teams of fishing vessels and policemen). Apparently, it was a typical stony or chondrite meteoroid. It began to be recorded by the satellite system at a height of 46 km and yielded bright bursts of radiation at heights of 34 and 28–25 km, i.e., it apparently broke up at these heights, We estimated the energy of these bolides by the same procedure [63, 78] as for the remaining bodies in Table 5, i.e., with the use of light curves recorded by satellite-based optical sensors. We note that analysis of the special features of entry, into the polar regions, of bolides that can serve as a trigger of intense auroral phenomena and magnetohydrodynamic phenomena seems a very important direction of subsequent investigations.

Šumava Bolide. Both the Prairic and European Networks recorded unusual bolides that flashed and disappeared at large heights, much higher than the typical values of 30–40 km. An example of such a meteoroid that broke up and yielded a bright "burst" at a large height is the Šumava bolide (EN 041274) [60]. It entered the atmosphere with a velocity of 27 km/sec and became visible at a height of 92 km. Four bright bursts were recorded. The first maximum was attained at a height of 75–76 km. The maximum brightness was (-21.5^{mag}) in the third burst at a height of 67 km. The bolide "disappeared" at a height of 58 km. At a height of 61 km, the velocity was still 23.7 km/sec, i.e., it was almost not retarded all the way to disappearance. According to evaluations [60] with the use of the radiation efficiencies common in meteoritics, the mass was 5 tons. No pronounced fragmentation was noted. The radiation spectrum consisted of numerous lines and corresponded approximately to a chondrite

composition. At the same time, the breakup occurred at a pressure of only 0.025–0.14 MPa, which leads us to the assumption of a cometary origin of this fragile body.

Modeling of the radiation spectrum for a large body [156] with the use of the absorption coefficients of the vapor of material with a composition that corresponds to the Halley comet [99] showed that on the whole it is similar to the spectrum of a chondrite meteoroid although the radiation efficiency of the former is somewhat lower. However had the meteoroid material represented pure aqueous ice, there would have been no numerous lines of metals and the radiation efficiency would have been an additional 2–3 orders of magnitude lower.

Evaluation of the radiation radius of the Šumava bolide [25] by the model of an evaporating piston [132] showed that its effective value increases in all bursts to 8–14 m (the rate of lateral expansion in the first burst is approximately 50-60 m/sec) and is a factor of 5–6 higher than that yielded by formula (8) with $k = 1$ (~ 10 m/sec). Thus, the "spreading" due to just a single aerodynamic load is incapable of providing an explanation for the high rate of expansion of the cloud of fragments and vapor. Apparently, only rapid and strong breakup of the Šumava meteoroid and a change in the evaporation mechanism itself can explain the high expansion rates. This was confirmed by calculations of [156], where quasivolumetric evaporation of the material was postulated.

Model of Meteoroid Breakup at Large Heights. According to [157], comets have a low density (0.1 ton/m^3) and a porous structure and are coated with an insulating layer formed due to loss of volatiles under the action of solar radiation. Its thickness depends on the duration of the revolution of the comet about the sun and the size of the body itself. For bodies with a size of the order of 1–3 m, it is about 1–4 cm [157]. These bodies apparently resemble a soiled city snowdrift that began to thaw in spring. The comet strength is estimated at a magnitude of only $5 \cdot 10^{-4}$ MPa. Aerodynamic loads of this order for the Šumava meteoroid are attained at a height of 80 km.

According to the model of [156], a porous body, under the action of aerodynamic forces, is compressed and acquires the shape of a thin disk. The density of the material in it becomes similar to the density of water, i.e., 1 ton/m^3, and the thickness is equal to 1/10 of the radius. As a consequence of the nonsphericity of internal inhomogeneities the actual motion is three-dimensional since the velocities of the material in the direction of motion on dissimilar radii become dissimilar. The disk breaks into fragments with a size of the order of its thickness, i.e., the characteristic number of large fragments is about 100. Of course, a much larger number of small fragments can occur. Hot air of the shock-compressed layer penetrates between them though originally with low velocities. The fragments begin to evaporate rapidly virtually throughout the volume.

Results of a two-dimensional calculation of a low-density spherical body being deformed under the action of aerodynamic forces [104] confirm the formation of a shell of compressed material that is broken up into a host of small fragments.

We note that at the large heights considered here the shock-compressed air is nonequilibrium. The ablating-piston model [132] allowed for only one form of nonequilibrium, namely, separation of the electron temperature from the ion temperature. More detailed allowance for the nonequilibrium in [158], taking into account the equation of chemical kinetics and the change in the charge composition, showed that the average parameters of the air are similar to those obtained within the framework of the equilibrium model. However, the difference in radiation is more significant. The plasma in the continuum is practically transparent and is mainly line in character, while the level populations are affected by intense luminescence. Even such details as allowing for multiplets separately or combining them into one level (as was done in [132]) turn out to be substantial [158]. Nonetheless, in both cases a major portion of the kinetic energy of the incoming air changes to radiation, mainly in the UV region. We are dealing with a radiation regime of flow [129, 130].

Sudden disappearance of a bolide at large heights can be due to total evaporation of the "crust," which has a decreased content of volatiles, and rapid disintegration of the "core," containing predominantly aqueous ice, frozen carbon dioxide, or ammonia which do not yield radiation as strong as the lines of metals.

Tunguska Event and the Meteoroid That Caused the Formation of Meteor Crater. The threshold of the dimensions of space bodies, starting with which the hazard due to asteroids and comets, from our viewpoint, becomes quite real, since the corresponding falls apparently will occur in the not very distant future (say, in 100–1000 years, and the probability of observing them amounts to 3–30% for our contemporaries, and the consequences of impacts are very significant), lies somewhere in the region of 30–100 m [1, 21]. The given estimate

of the probability, as is clear from the above, is very rough. Statistical data on large falls are obtained only in a large time interval, and furthermore, extrapolation of data from dimensions of 1–10 m, for which observational results are available, to the region of the indicated large dimensions is unreliable [63]. Practically the only experimental events that provide quite reliable information on large falls in the modern period are offered by the mentioned Tunguska event [31], the Sikhote-Alin "iron shower" [95, 147, 159], and the impact of the iron meteoroid that caused the formation of Meteor Crater [19]. In the latter event, because of the comparatively high strength of the iron meteoroid and the high density, breakup products struck the surface in the form of a rather compact mass in a zone smaller than the diameter of the crater formed, which was similar in dimensions to that which would have resulted from the impact of an unbroken body (unlike, say, the case of the fall of the Sikhote-Alin shower [95], where individual craters were much smaller than the dimensions of the crater field [31]). We note that the estimated [32] zone of breakup by the air shock wave in impact of the Meteor meteoroid is approximately the same as from the Tunguska air explosion [108].

If the Tunguska phenomenon is caused by a small comet, it seems that the pattern of its breakup and explosion is analogous in many respects to that for the Šumava meteoroid. A simple conversion of the breakup height by formula (12) from an initial size of 1 m to 30 m yields a change in the atmospheric density of 1000 times at the moment of total breakup, i.e., the corresponding height must decrease from 60 km to approximately 10 km. Estimates for the Tunguska event yield an explosion height of about 5–10 km [33]. Thus, the agreement is very good. However, it should be borne in mind that the similarity of (12) is, nonetheless, very approximate.

The Tunguska phenomenon could be induced by the fall not of a comet as was considered in [39, 40, 59] but of a stony asteroid, denser and stronger than a comet [34, 58]. However the question of why there are no meteorites or the traces of impacts of fragments against the earth's surface arises. An effort to answer it is made in [54, 55]: progressive crushing of the meteoroid led eventually to a very small size of the fragments and they evaporated by radiation both inside and outside a "fireball." In this case, the statistical character of the progressive-fragmentation model, which does not rule out that fragments could still be preserved, should be remembered. Thus, investigating both events of the Tunguska class and more recent phenomena of a smaller scale, in particular, the Šumava bolide, by numerical methods must be continued.

Plumes and Atmospheric Oscillations. A special feature of meteor explosions as compared to nuclear explosions is the presence, behind the body, of a rarefied layer, through which hot gas flows upward from denser atmospheric layers with an impurity of ablation products [1, 23, 160-162]. A "plume" occurs. Two-dimensional calculations [156] for the Šumava bolide, which exploded at heights larger than 60 km, showed that, in this case, the plume is ejected up to 140–180 km, i.e., into the ionosphere. In [163], attention was drawn to the fact that plume material, mainly air, ejected to large heights can be a hazard to low-orbit satellites.

Under gravity, the ejected material falls back. This gives rise to shock waves reflected from dense atmospheric layers and causes heating and fluctuation of the atmosphere [1, 23, 164]. The area spanned by these fluctuations corresponds originally to a radius of the order of the height of ascent and increases subsequently due to acoustic-gravitational waves [165-167].

Heating of the atmosphere in shock waves to temperatures of several thousand degrees gives rise to a prolonged pulse of IR radiation. With higher energies of the striker this radiation can even cause regional fires under the hot spot and global fires when the energies are very high. When the energies are comparatively low, this pulse is capable of ensuring detection of the impact.

The role of the trail is evaluated in [1]. Let energy release in the atmosphere occur predominantly on impact against the surface or as a result of fragmentation at height Z_*. The explosion energy is transferred to the air mass in a sphere of radius $H_* = H(Z_*)$. The characteristic internal energy of the heated gas is

$$e_* = E/\rho_* H_*^3. \tag{17}$$

Since the trail is a channel of strongly decreased density, for a large size of the body and accordingly a large channel width material heated in the explosion flies through the channel as through an empty tube with the velocity $V_* \approx \sqrt{2} e_*$. The gas ascends to the height

$$Z_{\max} = \frac{V_*^2}{2g} \sin^2 \theta = \frac{e_*}{g} \sin^2 \theta , \tag{18}$$

where θ is the slope of the trajectory and the rarefied channel to the horizon. This model was confirmed by two-dimensional calculations for a concentrated energy release. In [168-170], attention was drawn to the fact that plume formation begins even before the falling body is retarded and loses energy. Therefore the trail was modeled by the channel of a cylindrical explosion. The characteristic internal energy of the atmospheric gas heated in the trail in meteoroid flight turns out to be of the order of $V^2/2$.

The radius R_{ch} of the channel can be evaluated based on the cylindrical-explosion model:

$$R_{ch} = R\,(V/a_0)^{1/2} . \tag{19}$$

When $V = 30$ km/sec and $a_0 = 0.3$ km/sec we obtain $R_{ch} = 10R$.

A model of gas motion in the channel based on the assumption that the plume pressure eventually becomes equal to the ambient pressure was proposed in [118, 171]. The equation of motion of hot gas in a vertical channel has the following form:

$$\frac{du}{dt} = g\left[\frac{\rho_a}{\rho_0} \exp\left(-\frac{\gamma - 1}{\gamma H} Z\right) - 1\right] . \tag{20}$$

In deriving (20), the atmosphere was assumed to be exponential and the expansion of the gas in the channel was assumed to be adiabatic. In fact, the density of the air in the plume is governed by processes of not only adiabatic expansion but also radiation cooling, which is dissimilar at different heights. For bodies of different sizes, the density $\rho_a/\rho_0 \approx 1/10 - 1/30$ [25, 132].

For comparatively small bodies, R_{ch} is much smaller than the characteristic height of the atmosphere. In flowing through the trail from deep atmospheric layers, Calvin–Helmholtz instability and mixing of the hot gas of the trail and cold atmospheric gas can play a significant role. This process is enhanced due to the nonuniformity of energy release along the channel length as a result of multiple fragmentation of the body. Calculations [118, 171] showed that meteoroids with a radius of 1–3 m or smaller do not produce ballistic plumes. Bodies with a radius of 10–30 m (an event of the Tunguska-phenomenon class), conversely, can form plumes; however, their modeling requires special effort aimed at good spatial resolution of a long and comparatively thin trail and a correct description of the process of mixing at the boundary. Similar calculations for these sizes are very cumbersome and remain to be made.

When the energy release in the lower atmosphere is very powerful, oscillations of the upper atmosphere occur even in the absence of a trail. For example, in a 58 Mton nuclear explosion carried out in 1961 on New Land (Novaya Zemlya) at a height of 3.6 km, the shock wave decayed, but subsequently starting with a height of approximately 30 km it began to increase since it moved in a medium with a decreasing density. As calculations [1, 118] showed, acceleration of the shock wave gave rise to a powerful ascending motion behind it. The upward air flow began to be retarded by gravity, and subsequently a downward flow formed. The descending gas was retarded, colliding with dense layers, and caused heating and a pressure increase, which gave rise to an air counterflow. As a result shock waves (at heights of 100 km and higher) and large-scale nonlinear oscillations occurred that spanned, by times of 15 and 25 min, an area with radii of the order of 700 and 1200 km, respectively (with density disturbances of 50–100% and velocities of 0.5–1 km/sec). We note that calculations without allowance for a trail for the case of the fall of Comet Shoemaker–Levy 9 [172] provided a picture similar to the picture described, while the disturbances of Jupiter's upper atmosphere without allowance for a trail turned out to be much smaller than with allowance for it [173-175].

Of course, in the presence of a trail and a plume the occurrence of these oscillations is alleviated. If a fall occurred at an angle, the ballistic plume descending back induces oscillations far from the site of impact (for the Tunguska event, the flight velocity is estimated in [175] at 4.5 km/sec with the fall of the plume in the region of Baikal Lake).

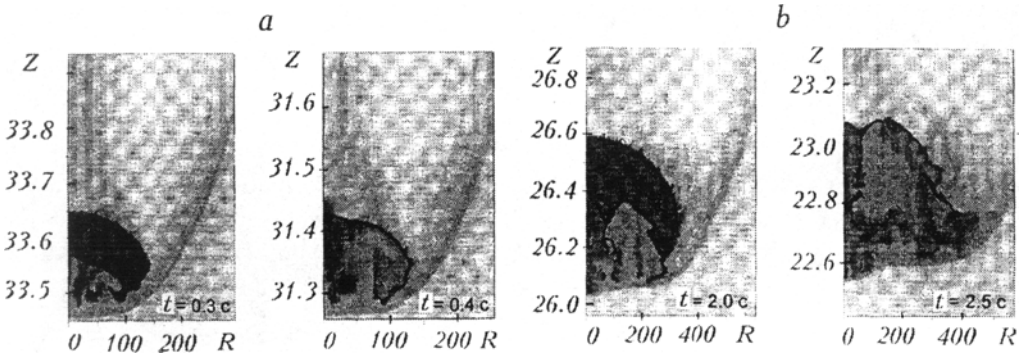

Fig. 4. Calculated density fields for comets with a radius of 160 m (a) and 345 m (b). The darker color corresponds to higher density. The zero time reference is for the position of the comets at a height of 40 km. Z, km; R, m.

Air layers at heights of $\geq 80-100$ km are ionized and their oscillations produce electrodynamic effects and magnetic disturbances. A magnetic signal with an amplitude of up to 90 gammas was recorded in Irkutsk [33, 176, 177] and lasted about 4 h. It was attributed to heating of air at large heights in ascent of a fireball and an explosion cloud and to a change in the conductivity and the current system in the ionosphere [176, 177]. According to [176], the refined time between the "explosion" [44, 46] and the onset of the magnetic disturbance is approximately 6 min, which for the distance of 900 km between Vanavara, where the epicenter of the explosion is located, and Irkutsk corresponds to a velocity of disturbance propagation in the horizontal direction of approximately 2.5 km/sec, and this is obviously larger than the velocity of acoustic-gravitational waves. It is, moveover, impossible to imagine transfer of the explosion cloud for distances as large as this in such a short time, as was assumed in [177]. However, this velocity is quite in agreement with that of the ballistic-plume model though with a slower one than in [175]. The time interval between the ascent and the descent of the air ejected back is in agreement with a vertical velocity of 1.5 km/sec. Incidentally, the ratio of the assessed values of the vertical and horizontal velocities corresponds approximately to a slope of the trajectory and, accordingly, the trail to the horizon of approximately 30°. The velocity of flight along the trajectory of 3 km/sec is somewhat lower than that obtained in [39], but at least it is not in contradiction with calculations of the ballistic-plume model.

Magnetohydrodynamic disturbances that propagate from the ionosphere to the magnetosphere are capable of causing a pouring out of fast particles from radiation belts and leading to auroral effects, i.e., to additional ionization. Blackouts on a regional and even global scale caused by impacts of meteoroids can be a hazard in our information age and deserve detailed investigation.

Calculation of the Entry of Very Low-Density Objects. In 1982, "atmospheric holes," i.e., dark spots with a characteristic size of about 50 km on the image of the earth's daytime glow in the ultraviolet, were detected using the photometer aboard the Dynamics Explorer 1 spacecraft [179]. They were interpreted by Frank as accumulations of water vapor above the zone of atmospheric glow, i.e., higher than 200 km. To explain the occurrence of the holes, hypotetical small comets with a mass of the order of 10–100 tons, whose structure, density, height, and causes of breakup in the rarefied atmosphere of the earth are unknown, were introduced. This report became the subject of agitated scientific discussion (see [157, 181] for a review of its initial stage). Some participants believe that the effect is attributable to an error in determination. However, measurements using the higher-precision equipment aboard the Polar spacecraft [182] seem to confirm the presence of small comets although the frequency of their fall is apparently much lower than was originally assumed [179, 180]. The problem has been discussed up to the present time (see, for example, [156, 183-185]), and this proves clearly what a long way we still are from understanding the structure and other properties of small comets (or fragments of large comets) as well as their interaction with the atmosphere.

There are different viewpoints as far as the density of the material of small comets is concerned. In [104], it is assumed to be very low – of the order of 10 kg/m^3, i.e., only a factor of 10 higher than the density of the atmosphere near the earth's surface. Upon compression to the normal density of water, the material was considered to be described by the equation of state of water. Two variants of calculating the motion of these bodies of large

TABLE 6. Sizes of Fragments of Comet Shoemaker–Levy 9

Fragment	No. of fragment	Upper limit of the radius, km	Size of R from the light curve, km	Class
A	21	0.5		2a
B	20	0.6		3
C	19	0.75		2a
D	18	0.5		3
E	17	1.0		2a
F	16	0.75		4
G2	15b	0.29		4
G1	15a	1.45	0.25 – 0.35	1
H	14	1.1	0.5	2a
K	12	1.35	0.4	1
L	11	1.25	0.7	1
N	9	0.5	0.15	3
P2	8b	0.7		4
Q2	7b	1.1		3
Q1	7a	1.45	0.25	2b
R	6	0.9	0.22–0.25	2b
S	5	1.55		2c
T	4	0.23		4
U	3	0.32		4
V	2	0.48		4
W	1	0.85	0.2	2c

dimensions were performed in [104]. The angle of entry was assumed to be 45°. With initial radii of spherical bodies of 345 and 160 m and velocities of 10 and 31.6 km/sec the kinetic energy in both cases was 20 Mton, i.e., it corresponded approximately to the kinetic energy of the Tunguska meteoroid. The calculation began from a height of 40 km. Figure 4 shows density fields at the instants when the cometary material is deformed intensely and the stage of explosion begins. It can be seen how the jets penetrate into the comet and dispersion of its material, mixing with air, rapid evaporation, and an explosion occur. For a body of approximately the same dimension (the radius is 200 m) but of much lower density, namely, 10^{-4} kg/m^3, the meteoroid mass is only 3 tons, i.e., it is similar to the mass for the Sumava meteoroid. This bolide explodes at a height of about 80 km, i.e., higher that actually occurred in observations. This sets a lower bound on the strength.

Fall of Fragments of Comet Shoemaker–Levy 9 on Jupiter. In analysis of the processes in entry of meteoroids into the earth's atmosphere we cannot disregard data obtained for other planets of the earth group that have an atmosphere, namely, Venus and Mars, and, of course, unique data obtained recently when Comet Shoemaker–Levy 9 struck the giant gas planet Jupiter – a remarkable event in the history of astronomy and meteoritics. When Comet Shoemaker–Levy 9 passed Jupiter in July, 1992 it fractured under the action of tidal forces, and 21 fragments were formed [187]. Fragments of the comet were first detected in July, 1993 and were watched in a telescope till their fall in mid-July, 1994 [188]. The fragments were surrounded by a great deal of dust, and therefore only an upper estimate of their possible dimensions is available. It and the class of the consequences of the impact, according to data of the Hubble space telescope [169], are given in Table 6. Class 1 corresponds to a dimension of the disturbed region on the surface of more than 10,000 km and to several wave rings diverging from the site of impact. Class 2a corresponds to dimensions of the disturbed region of 4000 to 6000 km and, possibly to several waves. In class 2b, the waves are single. In class 3, the dimension is < 3000 km; there are no waves. The sites of the falls of fragments F, P2, T, and U were not detected at all (class 4). The sites of the falls of fragments J (13), M (10), and P1 (8a) disappeared from the field of view in Jupiter rotation shortly after the impact and therefore were not analyzed and are not given in the table.

For fragments A, E, G, and W, the heights of the plumes that occurred were determined with time [189]. The maximum height was 3300 and 2100 km for fragments G and W and about 2800 km for A and E. Originally it was assumed to determine the kinetic energy and the size of the striker from the plume height [168, 190];

however, subsequently it became clear [169] that this height depends weakly on the size since the depths of penetration and the main energy release vary strongly. The upper part of the plume results from the escape of gas from the hot trail that is formed behind the fragment at large heights and has approximately the same temperature and, accordingly, velocity of escape for all the fragments, and it is governed mainly by the impact velocity.

The dimensions of the fragments were determined by comparing light curves recorded on the Galileo spacecraft with theoretical curves [109, 110, 191]. The latter were obtained by solving a number of variants of two-dimensional and three-dimensional radiation-gasdynamic problems, in which detailed tables of the optical properties of Jupiter's atmosphere and cometary vapor were used and deformation of the fragments due to aerodynamic forces and their evaporation by radiation were allowed for. The sizes obtained in this manner are given in the next to last column of Table 6. As is evident, they are 0.25–0.7 km.

The first value for fragment G1 is obtained [109, 110] from the initial portion of the light curve recorded on the Galileo spacecraft for $\lambda = 0.438$ μm, and the second – from the luminosity maximum for $\lambda = 0.292$ nm in the bolide stage of entry into the atmosphere. The values for fragments L, H, and Q1 are obtained from the light curves for $\lambda = 0.945$ nm, and for K, W, and N – for $\lambda = 0.89$ nm. The fragment R is determined from an infrared-radiation pulse ($\lambda = 2.3$, 3.5, and 4.5 μm) of duration of 10 min that was recorded using a Keck ground-based telescope and corresponds to the stage of the fall of a ballistic plume onto Jupiter's atmosphere [192].

The sizes determined from the light curve are smaller, on the average, by a factor of 2–4 than the sizes found in astronomical observations before the fall. This is due to the fact that the central portion of a fragment was surrounded by an extended dusty coma.

We note that the radiation radius, i.e., the size of the effective body that yields the radiation intensities observed, is larger by approximately a factor of 3 than the size of the fragment itself. This is due to the fact that pairs formed at a height of 150–200 km move downward together with the body, remaining rather cold (of the order of the phase-transition temperature) and dense. The effective radius turns out to be much larger than it would be in the absence of ablation.

Thus, under conditions of intense ablation of the meteoroid at large heights, use of quasistationary solutions of problems of flow for smaller heights where the evaporation intensity is already low with allowance only for "local" masses of the vapor formed at these smaller heights is invalid. The problem of entry as a whole is substantially nonstationary.

Because of the large dimensions of the body the radiation is emitted mainly by an optically dense shock wave. Incidentally, this makes it impossible to simply use empirical data on the radiation efficiency of bright earth bolides [60] since radiation even for the largest earth meteors of those recorded thus far occurs mainly in lines and bands and the role of the continuum becomes pronounced only for deep-penetrating meteors.

In dense atmospheric layers near a cloudy layer, where evaporation almost ceases, the vapor mass evaporated earlier is retarded and is removed by the flow. The trail at these heights corresponds to the actual size of the body and becomes much thinner. However in deeper layers it increases again due to intense fragmentation.

The characteristic height of Jupiter's atmosphere above the clouds is approximately 24–30 km. This is larger by approximately a factor of 2.5–3 than for the earth. Based on similarity relation (12), the processes of entry of fragments with dimensions of 0.25–0.7 km into Jupiter's atmosphere are considered to model, as a first approximation, the processes of entry of a meteoroid with a dimension of 0.08–0.2 km into the earth's atmosphere. Thus, it is likely that these meteoroids will reach the earth's surface, which is in agreement with theoretical evaluations based on liquid models [1, 78]. When these bodies enter the earth's atmosphere a plume, a hot spot in its return-fall, and intense waves that propagate radially in the upper atmosphere occur.

We note that when the fragments of Comet Shoemaker–Levy 9 were falling on Jupiter auroral effects were also observed in regions magnetoconjugate to the sites of impact, which confirms the possibility of magneto-hydrodynamic effects in impact against the earth's atmosphere, too. Furthermore, for the earth, they must be much stronger since the magnetic field of Jupiter is very strong (stronger by approximately an order of magnitude than the earth's field) and the energy of Jupiter's magnetosphere, roughly speaking, is 5 orders of magnitude higher than the energy of the earth's magnetosphere.

The motion and breakup of very large meteoroids in the extended and dense atmosphere of Venus [77, 193] can also be considered as a model of the motion of smaller bodies in the earth's atmosphere [1]. However, falls of large meteoroids are very rare. At the same time, falls of comparatively small bodies on Mars with its rarefied atmosphere are much more frequent (thus, Benešov-type meteoroids fall approximately 10–20 times a year [194]). Fragments of Benešov-type meteoroids reach the surface of Mars [194]. According to the hypothesis [195], even without reaching the surface or "exploding" near it, they can cause local dust storms that can serve as good indicators of falls, just like virgin craters and "bursts." Observations on Mars and other planets are more expensive than the corresponding observations on the earth. Therefore it is appropriate first to augment and improve the systems of both ground-based and satellite observations of the entry of meteoroids into the earth's atmosphere.

Interaction of a Cloud and Small Particles with the Atmosphere. As a result of action exerted on an asteroid or a comet with the aim of eliminating the hazard due to asteroids or comets these objects can be broken up to the state of sand grains or even fine dust ("pulverization") [196, 197]. However, small particles, too, penetrating abundantly into the earth's atmosphere, cause heating of it, intense radiation, and the formation of a shock wave. These factors can turn out to be very hazardous, including the capacity for being global in character, since the action of a cloud will be exerted on a large area. If the size of the cloud is much larger than several characteristic heights the problem can be considered to be two-dimensional [199-200]. The physical model is similar to the sand-bag model in many respects [78, 119, 122]; however, there also are differences. In the evaporation model [197, 198], allowance is made for removal of mass by ablation (in the presence of a strong difference between the particle velocity and the velocity of the ambient air and vapor) and separately by the thermal radiation of the entire "fireball." In the first case, use is made of the empirical ablation coefficient obtained for meteoroids that move in cold air with hypersonic velocities. In the second case, the radiation heat flux in [199] is calculated under the assumption that the thermodynamic and optical properties of the vapor are the same as for atmospheric air. However, data on the optical characteristics of the vapor [99] and calculations of radiation transfer in a shock-compressed layer of air and vapor [132] show that this assumption is very far from the truth.

To calculate the motion of a compact cloud in the atmosphere, a two-dimensional problem for particles with a radius of 0.1–1 mm was solved in [89]. For a cloud with an initial size of 1 km, a bulk concentration of the particles of 10^{-4}, and a velocity of 20 km/sec, the kinetic energy was about 18 Mton in TNT equivalent, which is of the order of the energy of the space body that caused the Tunguska phenomenon. The interphase interaction led to rapid equalization of the velocities of the particles and the gas, i.e., these small particles evaporate mainly by thermal radiation. The cloud of particles and vapor acquired the shape of a torus (a breakthrough at the center, as in the calculations of [119, 124]). The particles disappeared at a height of 30 km, while the vapor was retarded at a height of 20 km. The height at which explosion-like expansion occurs turns out to be substantially larger than the estimate typical of the Tunguska event [33]. However, the amplitude of the shock wave that reaches the earth's surface turned out to be rather large, namely, 1.3 MPa/m^2. Thus, the increase in the explosion height as compared to that for the Tunguska phenomenon is not so significant as to avoid the action of the shock wave and fires but the area of burn increases and the zone of the initial disturbance of the ionosphere also expands. Therefore disintegration of a meteoroid to the state of fine dust can sometimes lead to enhancement of the action rather than to its attenuation. In this connection, a deviation of the trajectory of a hazardous meteoroid from the earth can turn out to be a more rational strategy for eliminating an asteroid hazard with nonnuclear means [201, 202].

Unfortunately, it is apparently impossible to use some methods of step-by-step action (a solar sail, collimators of solar radiation for evaporation, low-drive motors, etc.) for bodies of small dimensions since they are detected in a telescope or using radar units at comparatively small distances from the earth, and there is not enough time to implement the indicated types of "mild" action. For rapid action at distances of only tens of millions of kilometers from the earth with the use of nuclear means, heavy rockets with nuclear charges must be on duty on it [203, 204]. However, in this case, the occurrence of compact dust formations arriving at the earth's atmosphere is not improbable while the maintenance of nuclear arsenals is hazardous by itself.

Therefore it is desirable to implement rather intense actions that lead to a deviation of the cloud of fragments from the earth (for example, using focused laser or superhigh-frequency radiation [202]). But in

developing the methods (and means) of these actions, it is necessary to obtain detailed information on the space bodies themselves or at least on possible limits of variation of their properties.

Conclusion. As follows from the above, data and theoretical calculations of the entry of large meteoroids into the earth's atmosphere available at present are scanty and incomplete as yet; however they provide an idea of the main processes occurring and make it possible to assess the basic parameters. Further accumulation of observational data and their analysis as well as the development of theoretical models and calculations by them, primarily to compare with observational data and to analyze new effects not investigated in detail earlier (for example, electro- and magnetohydrodynamic disturbances), are required.

NOTATION

m_v, bolide brightness in stellar quantities; I, radiation intensity; I_{max}, maximum radiation intensity; M, meteoroid mass; S, cross-sectional area; V, velocity of the body along the trajectory; C_D, coefficient of resistance; t, time; ρ_a, atmospheric density at the height Z; ρ_0, meteoroid density; ρ_*, air density at the breakup height; ρ_a^0, air density at the earth; θ, slope of the trajectory to the horizon; Z_B, initial point of the trajectory; Z_R, zenith distance; Z_{max}, maximum height of ascent of the plume; V_B, initial velocity; V_E, final velocity; m_a, specific mass of the atmosphere above the level Z; φ, dimensionless coefficient of decrease in strength; σ, meteoroid strength; σ_s, strength of a specimen of mass m_s; u, velocity in the lateral direction; k, numerical coefficient of the order of unity; E_k, kinetic energy in kton in TNT equivalent; E_r, radiation energy; g, free-fall acceleration; R_0, initial radius of the meteoroid; R, radius of the body; a_0, velocity of sound in undisturbed air; γ, adiabatic exponent; R_{ch}, radius of the channel; m_0, specific mass of the meteoroid; m_{max}, maximum brightness in stellar quantities; H_B, height of appearance of the bolide; H_{max}, maximum-intensity height; H_E, final height; H, characteristic height of the atmosphere; α, exponent in the law of decrease in strength as the mass increases; η, efficiency of the changeover of kinetic energy to radiation energy; η_i, integral (over the entire flight time) radiation efficiency; M_{ph}, photometric mass; M_B and M_E, initial and finite dynamic masses; M_r, radiation mass; M_0, estimate of the mass of satellite bolides; N, number of falls of meteoroids with an energy higher than E_k in a year on the entire earth; N_m, number of fragments; e_*, characteristic internal energy of heated gas; d, distance between fragments of radius R. Subscripts and superscripts: v, visual; 0, initial; D, resistance; E, end; a, air; B, beginning; max, maximum; t, tangential; c, compression; s, small specimen; *, characteristic quantities; R, radiant; ch, channel.

REFERENCES

1. V. V. Adushkin and I. V. Nemchinov (Nemtchinov), in: T. Gehrels (ed.), *Hazards due to Comets and Asteroids*, Tucson and London (1994), pp. 721-778.
2. D. Morrison, C. R. Chapman, and P. Slovic, in: T. Gehrels (ed.), *Hazards due to Comets and Asteroids*, Tucson and London (1994), pp. 59-93.
3. Z. Ceplecha, P. Spurný, J. Bozek, et al., *Bull. Astron. Inst. Czechosl.*, **38**, No. 4, 211-222 (1987).
4. P. Spurný, *SPIE's Int. Symp. on Optical Sci. Engn. and Instrumentation Conf.*, Paper 3116B, San Diego (1997).
5. J. Oberst, S. Molau, D. Heinlein, et al., *Meteoritics and Planetary Sci.*, **33**, 49-56 (1998).
6. Z. Ceplecha, *Bull. Astron. Inst. Czechosl.*, **12**, 21-49 (1961).
7. R. E. McCrosky, A. Posen, G. Schwartz, and C.-Y. Shao, *J. Geophys. Res.*, **76**, No. 17, 4090-4108 (1971).
8. I. Halliday, A. A. Griffin, and A. T. Blackwell, *Meteoritics*, **16**, No. 2, 153-170 (1981).
9. Z. Ceplecha, P. Spurný, J. Borovička, and J. Keklikova, *Astron. Astrophys.*, **279**, 615-626 (1993).
10. J. Borovička, O. P. Popova, I. V. Nemchinov (Nemtchinov), et al., *Astron. Astrophys.*, **334**, 713-738 (1998).
11. Z. Ceplecha, *Astron. Astrophys.*, **311**, 329-332 (1996).
12. H. Campins and T. D. Swindle, *Meteoritics and Planetary Sci.*, **33**, 1201-1211 (1998).
13. M. R. Rampino and B. M. Haggerty, in: T. Gehrels (ed.), *Hazards due to Comets and Asteroids*, Tucson and London (1994), pp. 827-857.
14. J. Smit, in: T. Gehrels (ed.), *Hazards due to Comets and Asteroids*, Tucson and London (1994), pp. 859-878.

15. A. Carusi, T. Gehrels, E. F. Helin, et al., in: T. Gehrels (ed.), *Hazards due to Comets and Asteroids*, Tucson and London (1994), pp. 127-147.
16. E. Bowell and K. Muinonen, in: T. Gehrels (ed.), *Hazards due to Comets and Asteroids*, Tucson and London (1994), pp. 149-197.
17. J. V. Scotti, D. Rabinowitz, and B. Marsden, *Nature*, **354**, No. 6351, 287-289 (1993).
18. J. V. Scotti, in: A. Milani, M. D. Martino, and A. Cellino (eds.), *Asteroids, Comets, Meteors*, Kluwer, Dordrecht (1994), pp. 17-30.
19. H. Melosh, *Formation of Impact Craters: A Geological Process* [Russian translation], Moscow (1994).
20. A. V. Vityazev and G. V. Pechernikova, *Asteroid and Seismic Hazards* [in Russian], Moscow (1997).
21. J. Hills, I. V. Nemchinov (Nemtchinov), S. P. Popov, and A. V. Teterev, in: T. Gehrels (ed.), *Hazards due to Comets and Asteroids*, Tucson and London (1994), pp. 779-789.
22. I. V. Nemchinov (Nemtchinov), T. V. Loseva, and A. V. Teterev, *Earth, Moon and Planets*, 72, 405-418 (1996).
23. I. V. Nemchinov, T. V. Loseva, and V. V. Shuvalov, in: *Dynamic Processes in Geospheres: Geophysics of Strong Disturbances,* Collection of Scientific Papers of the Institute of the Dynamics of the Geospheres, Russian Academy of Sciences, Moscow (1994), pp. 205-219.
24. S. Yabushita and N. Hatta, *Earth, Moon and Planets*, **65**, 7-13 (1994).
25. I. V. Nemchinov (Nemtchinov), O. P. Popova, V. V. Shuvalov, and V. V. Svetsov, *Planet. Space Sci.*, **42**, No. 6, 491-506 (1994).
26. A. V. Teterev, L. V. Rudak, N. I. Misyuchenko, and G. S. Romanov, in: *Abstr. of Papers Submitted to the IVth Interstate Symp. on Radiation Plasmadynamics* [in Russian], Moscow (1997), pp. 229-230.
27. L. V. Shurshalov, *Zh. Vych. Mat. Mat. Fiz.*, **36**, No. 6, 924-933 (1986).
28. S. Glasstone and J. Dolan, *The Effects of Nuclear Weapons*, Governm. Print. Office, Washington, DC (1977).
29. T. V. Loseva, I. B. Kosarev, and I. V. Nemchinov (Nemtchinov), *Astron. Vestn.*, **32**, No. 2, 169-176 (1998).
30. E. Shoemaker, *Ann. Rev. Earth Planet. Sci.*, **11**, 461-494 (1993).
31. E. L. Krinov, *Tunguska Meteorite* [in Russian], Moscow–Leningrad (1949).
32. D. A. Kring, *Meteoritics and Planetary Sci.*, **32**, 517-530 (1997).
33. N. V. Vasil'ev (Vasilyev), *Planet. Space Sci.*, **46**, No. 2/3, 129-150 (1998).
34. C. F. Chyba, P. J. Thomas, and K. J. Zahnle, *Nature*, **361**, No. 6407, 40-44 (1993).
35. V. P. Korobeinikov, P. I. Chushkin, and L. V. Shurshalov, *Acta Astronautica*, **9**, No. 10, 641-643 (1982).
36. I. G. Zotkin and M. A. Tsikulin, *Dokl. Akad. Nauk SSSR*, **167**, No. 1, 59-62 (1966).
37. M. A. Tsikulin, *Shock Waves in the Motion of Large Meteoric Bodies in the Atmosphere* [in Russian], Moscow (1969).
38. V. P. Korobeinikov, S. B. Gusev, P. I. Chushkin, and L. V. Shurshalov, *Computers Fluids*, **21**, No. 3, 323-330 (1992).
39. V. P. Korobeinikov, P. I. Chushkin, and L. V. Shurshalov, in: *Interaction of Meteoric Material with the Earth* [in Russian], Novosibirsk (1980), pp. 115-137.
40. V. P. Korobeinikov, P. I. Chushkin, and L. V. Shurshalov, *Astron. Vestn.*, **25**, No. 3, 327-343 (1991).
41. V. G. Fast, *Problem of the Tunguska Meteorite* [in Russian], Tomsk, Issue 2, 40-61 (1967).
42. R. P. Turco, O. Toon, C. Park, et al., *Icarus*, **50**, 1-52 (1982).
43. J. N. R. Hunt, R. Palmer, and W. Penney, *Phil. Trans. Roy. Soc.*, (London), Ser. A, **252**, No. 1011, 275-315 (1960).
44. I. P. Pasechnik, in: *Space Matter on the Earth* [in Russian], Novosibirsk (1976), pp. 25-54.
45. A. Ben-Menahem, *Phys. Earth and Planet. Interiors*, **11**, 1-35 (1975).
46. F. J. W. Whipple, *Quart. J. Roy. Meteorolog. Soc.*, **60**, 505-515 (1930).
47. J. Rahe, V. Vanysek, and P. R. Weissman, in: T. Gehrels (ed.), *Hazards due to Comets and Asteroids*, Tucson and London (1994), pp. 597-634.
48. F. J. W. Whipple, *Astrophys. J.*, **112**, 375-394 (1950).
49. F. J. W. Whipple, *Astrophys. J.*, **113**, 464-474 (1951).

50. B. Donn, in: R. L. Newburn, Jr., M. Nengebauer, and J. Rehe (eds.), *Comets in the Post-Halley Era*, Kluwer, Dordrecht (1991), pp. 335-359.
51. P. R. Weissman, *Nature*, **320**, 242-244 (1984).
52. T. I. Gambosi and H. L. F. Houpis, *Nature*, **324**, 43-46 (1986).
53. V. G. Fesenkov, *Astron. Zh.*, **38**, No. 4, 577-592 (1961).
54. V. V. Svetsov, *Nature*, **383**, No. 6602, 697-699 (1996).
55. V. V. Svetsov, *Planet. Space Sci.*, **46**, No. 2/3, 261-268 (1998).
56. S. S. Grigoryan (Grigorian), *Planet. Space Sci.*, **46**, No. 2/3, 213-217 (1998).
57. S. S. Grigoryan, *Dokl. Akad. Nauk SSSR*, **231**, No. 1, 57-60 (1976).
58. Z. Sekanina, *Planet. Space Sci.*, **46**, No. 2/3, 191-204 (1998).
59. D. J. Asher and D. I. Stell, *Planet. Space Sci.*, **46**, No. 2/3, 20-23 (1998).
60. J. Borovička and P. Spurný, *Icarus*, **121**, 484-510 (1996).
61. J. Borovička, O. P. Popova, A. P. Golub', et al., *Astron. Astrophys.*, **337**, 591-602 (1998).
62. I. V. Nemchinov (Nemtchinov), C. Jacobs, E. Tagliaferri, et al., in: J. L. Remo (ed.), *Near-Earth Objects*, Annals of the New York Acad. Sci., Vol. 822, New York (1997), pp. 303-317.
63. I. V. Nemchinov (Nemtchinov), V. V. Svetsov, I. B. Kosarev, et al., *Icarus*, **130**, 259-274 (1997).
64. D. A. Reynolds, in: G. H. Canavan, J. C. Solem, and J. D. G. Rather (eds.), *Near-Earth-Object Interception Workshop*, Los Alamos (1992), pp. 221-226.
65. E. Tagliaferri, R. Spalding, C. Jacobs, et al., in: T. Gehrels (ed.), *Hazards due to Comets and Asteroids*, Tucson and London (1994), pp. 199-220.
66. Z. Ceplecha, *Astron. Astrophys.*, **263**, 361-366 (1992).
67. Z. Ceplecha, *SPIE's Int. Symp. on Optical Sci. Engn. and Instrumentation Conf.*, Paper 3116B, San Diego (1997).
68. B. Baldwin and Y. Sheafler, *J. Geophys. Res.*, **76**, 4653-4668 (1971).
69. E. A. Krinov, *Meteoritika*, Issue 9, 215-262 (1974).
70. Q. R. Passey and H. J. Melosh, *Icarus*, **42**, No. 2, 211-233 (1980).
71. H. J. Melosh, *Multiring Basins*, in: *Proc. Lunar Planet. Sci. Conf.*, Vol. 12A (1981), pp. 29-35.
72. V. A. Bronshtén, *Astron. Vestn.*, **28**, No. 2, 118-124 (1994).
73. V. A. Bronshtén, *Astron. Vestn.*, **29**, No. 5, 450-459 (1995).
74. S. S. Grigoryan, *Kosm. Issled*, **17**, No. 6, 875-893 (1979).
75. N. A. Artem'eva and V. V. Shuvalov, *Shock Waves*, **5**, No. 6, 359-367 (1996).
76. B. A. Ivanov, *Lunar and Planet. Sci.* (Houston), **XIX**, 535-536(1988).
77. A. T. Bazilevsky, B. A. Ivanov, G. A. Burba, et al., *J. Geophys. Res.*, **92**, 12869-12901 (1987).
78. V. V. Svetsov, I. V. Nemchinov (Nemtchinov), and A. V. Teterev, *Icarus*, **116**, No. 1, 131-153 (1995).
79. A. A. Amsden, H. M. Ruppel, and C. W. Hirt, *SALE: a Simplified ALE Computer Program for Fluid Flow at All Speeds*, Los Alamos Nat. Lab. Report LA-8095, Los Alamos, New Mexico (1980).
80. H. J. Melosh, E. V. Ryan, and E. Asphaug, *J. Geophys. Res.*, **97**, 14735-14759 (1992).
81. V. A. Ivanov, D. Deniem, and G. Neukum, *Int. J. Impact Engn.*, **20**, 411-430 (1997).
82. V. A. Ivanov, A. T. Bazilevsky, and G. Neukum, *Planet. Space Sci.*, **451**, 993-1007 (1997).
83. D. E. Grady and M. E. Kipp, *Int. J. Rock Mech. Miner. Sci. Geomech. Abstr.*, **17**, 147-157 (1980).
84. W. Weibull, *Proc. Roy. Swedish Inst. Engn. Res.*, **151**, 1-45 (1939).
85. W. Weibull, *J. Appl. Mech.*, **10**, 140-141 (1951).
86. V. P. Korobeinikov, S. B. Gusev, and I. V. Semenov, *Astron. Vestn.*, **31**, No. 4, 370-384 (1997).
87. V. I. Tsvetkov and A. Ya. Skripnik, *Astron. Vestn.*, **25**, No. 3, 364-371 (1991).
88. R. P. Medvedev, R. F. Gorbatsevich, and I. T. Zotkin, *Meteoritika*, Issue 44, 105-110 (1985).
89. P. V. Plotnikov and L. V. Shurshalov, *Astron. Vestn.*, **31**, No. 1, 72-81 (1997).
90. K. Fukushima, in: A. P. Cunha (ed.), *Scale Effects in Rock Masses*, Balkemo, Rotterdam (1990), pp. 209-219.
91. A. Fujiwara, P. Cerroni, D. Davis, et al., in: R. P. Binzel, T. Gehrels, and M. S. Mathews (eds.), *Asteroids I*, Tuscon (1989), pp. 240-265.

92. P. Jenniskens, H. Betlem, J. Betlem, et al., *Meteoritics*, **29**, No. 2, 246-254 (1994).
93. A. G. Ivanov and V. A. Ryzhanskii, *Dokl. Ross. Akad. Nauk*, **353**, No. 3, 334-337 (1997).
94. J. G. Hills and M. P. Goda, *Astron. J.*, **103**, 1114-1144 (1993).
95. I. V. Nemchinov and O. P. Popova, *Astron. Vestn.*, **31**, No. 5, 458-471 (1997).
96. I. A. Dubrovina and V. P. Stulov, *Vestn. Mosk. Univ., Ser. 1, Matematika, Mekhanika*, No. 5, 46-49 (1989).
97. N. A. Artem'eva, I. A. Trubetskaya, and V. V. Shuvalov, in: *Dynamic Processes in the Earth's Inner and Outer Shells (Geophysics of Strong Disturbances)*, Collection of Scientific Papers of the Institute of the Dynamics of the Geospheres, Russian Academy of Sciences [in Russian], Moscow (1995), pp. 99-113.
98. N. A. Artem'eva and V. V. Shuvalov, in: *Joint Europ. Nat. Astron. Meeting for 1998 (JENAM-98)*, Prague (1998), p. 65.
99. I. B. Kosarev, T. V. Loseva, and I. V. Nemchinov, *Astron. Vestn.*, **30**, No. 4, 307-320 (1996).
100. P. H. Shultz and S. Sugita, *Lunar and Planet. Sci.* (Houston), **XXV**, 1215-1216 (1994).
101. J. S. Dohnanyi, *J. Geophys. Res.*, **74**, 2531-2554 (1969).
102. V. M. Hazins and V. V. Svetsov, *J. Comput. Phys.*, **105**, 187-198 (1993).
103. A. V. Teterev, N. I. Misychenko, L. V. Rudak, et al., *Lunar and Planet. Sci.* (Houston), **XXIV**, 1417-1418 (1992).
104. A. V. Teterev, *Lunar and Planet. Sci.* (Houston), **XXIX**, 1578 (1998).
105. A. V. Teterev, in: *Proc. 2nd Int. Conf. on Finite-Difference Methods: Theory and Applications*, Vol. 3, Minsk (1998), pp. 103-110.
106. S. M. Bakhrakh, Yu. P. Glagoleva, M. S. Samigulin, et al., *Dokl. Akad. Nauk SSSR*, **257**, 566-569 (1981).
107. C. W. Hirt and B. D. Nichols, *J. Comput. Phys.*, **39**, 201-295 (1981).
108. I. V. Nemchinov, N. A. Artem'eva, I. B. Kosarev, et al., in: *Dynamic Processes in the Earth's Inner and Outer Shells (Geophysics of Strong Disturbances)*, Collection of Scientific Papers of the Institute of the Dynamics of the Geospheres, Russian Academy of Sciences [in Russian], Moscow (1995), pp. 88-98.
109. I. V. Nemchinov (Nemtchinov), V. V. Shuvalov, I. B. Kosarev, et al., *Planet. Space Sci.*, **45**, No. 3, 311-326 (1997).
110. V. V. Shuvalov, N. A. Artem'eva, I. B. Kosarev, et al., *Astron. Vestn.*, **31**, No. 5, 441-449 (1997).
111. V. V. Shuvalov and N. A. Artem'eva, *Astron. Vestn.*, **32**, No. 5, 445-454 (1998).
112. V. V. Shuvalov, "3D hydrodynamic code SOVA for interfacial flows. Application to thermal layer effect," *Shock Waves* (1999) (in press).
113. J. M. McGlaun, S. L. Thompson, and M. G. Elrick, *Int. J. Impact Engn.*, **10**, 351-360 (1990).
114. O. P. Popova and V. V. Svetsov, in: *Dynamic Processes in the Earth's Inner and Outer Shells (Geophysics of Strong Disturbances)*, Collection of Scientific Papers of the Institute of the Dynamics of the Geospheres, Russian Academy of Sciences [in Russian], Moscow (1995), pp. 120-127.
115. V. Svetsov, O. Popova, V. Rybakov, et al., *Shock Waves*, 7, 325-334 (1997).
116. V. V. Adushkin, Yu. I. Zetser, Yu. N. Kiselev, et al., *Dokl. Ross. Akad. Nauk*, **331**, No. 4, 155-158 (1993).
117. A. P. Golub', Yu. N. Kiselev, I. V. Nemchinov, et al., in: *Physical Processes in Geospheres with Strong Disturbances (Geophysics of Strong Disturbances)*, Collection of Scientific Papers of the Institute of the Dynamics of the Geospheres, Russian Academy of Sciences [in Russian], Moscow (1997), pp. 179-197.
118. V. V. Shuvalov, *Dynamic Processes in the Atmosphere Induced by Strong Pulsed Disturbances*, Author's Abstract of Doctoral Dissertation (in Physical and Mathematical Sciences), Moscow (1999).
119. A. V. Teterev and I. V. Nemchinov (Nemtchinov), *Lunar and Planet. Sci.* (Houston), **XXIV**, 1415-1416 (1993).
120. J. D. O'Keefe and T. J. Ahrens, *J. Geophys. Res.*, 87, 6668-6680 (1982).
121. A. V. Teterev, in: *Abstr. of Papers Submitted to the IVth Interstate Symp. on Radiation Plasmadynamics*, Moscow (1997), pp. 93-94.
122. A. V. Teterev, *Lunar and Planet. Sci.* (Houston), **XXIX**, 1276 (1998).
123. R. E. McCrosky, C.-Y. Shao, and A. Posen, *Prairic Network Fireball Data I. Summary and Orbits*, Preprint Ser. 665 of the Smithsonian Center for Astrophys., Washington, DC (1976).
124. R. E. McCrosky, C.-Y. Shao, and A. Posen, *Prairic Network Fireball Data II. Trajectories and Light Curves*, Preprint Ser. 721 of the Smithsonian Center for Astrophys., Washington, DC (1977).
125. R. E. McCrosky, C.-Y. Shao, and A. Posen, *Meteoritika*, Issue 37, 44-59 (1978).
126. V. A. Bronshtén, *Physics of Meteoric Phenomena* [in Russian], Moscow (1981).

127. J. J. Givens and W. A. Page, *J. Geophys. Res.*, 76, 1039-1054 (1971).
128. Ya. B. Zel'dovich and Yu. P. Raizer, *Physics of Shock Waves and High-Temperature Hydrodynamic Phenomena* [in Russian], Moscow (1966).
129. Yu. N. Kiselev, I. V. Nemchinov, and V. V. Shuvalov, *Zh. Vych. Mat. Mat. Fiz.*, **31**, No. 6, 901-921 (1991).
130. I. V. Nemchinov, *Khim. Fiz.*, **12**, No. 3, 320-333 (1993).
131. I. V. Nemchinov, V. V. Novikova, and O. P. Popova, *Meteoritika*, Issue 48, 124-136 (1989).
132. A. P. Golub', I. B. Kosarev, I. V. Nemchinov, and V. V. Shuvalov, *Astron. Vestn.*, **30**, No. 3, 183-197 (1996).
133. G. G. Chernyi, *Flow of Gas with a High Supersonic Velocity* [in Russian], Moscow (1959).
134. W. D. Hays and R. F. Probstein, *Theory of Hypersonic Flows* [Russian translation], Moscow (1962).
135. I. V. Avilova, L. M. Biberman, V. S. Vorob'ev, et al., *Optical Properties of Hot Air* [in Russian], Moscow (1990).
136. E. Jarosewitch, *Meteoritics*, **25**, No. 4, 323-337 (1990).
137. E. K. Jessberger and J. Kissel, in: R. L. Newburn, Jr., M. Nengebauer, and J. Rehe (eds.), *Comets in Post-Halley Era*, Vol. 2, Kluwer, Dordrecht (1991), pp. 1075-1092.
138. O. P. Popova and I. V. Nemchinov (Nemtchinov), *Meteoritics and Planetary Sci.*, **31**, A110, supplement (1996).
139. D. O. ReVelle, *J. Atmosph. Terr. Phys.*, **41**, No. 5, 453-473 (1979).
140. D. O. ReVelle, *J. Geophys. Res.*, **85**, No. B4, 1803-1809 (1980).
141. Z. Ceplecha, *Brief Report on Light Curves of PN Fireballs* (1995) (personal communication).
142. Z. Ceplecha, J. Borovička, W. G. Elford, et al., *Space Sci. Rev.*, **84**, 327-471 (1998).
143. P. Brown, Z. Ceplecha, R. L. Hawkes, et al., *Nature*, **367**, 624-626 (1994).
144. I. Halliday, A. A. Griffin, and A. T. Blackwell, *Meteoritics and Planetary Sci.*, **31**, No. 2, 185-217 (1996).
145. D. O. ReVelle, in: J. L. Remo (ed.), *Near-Earth Objects*, Annals of the New York Acad. Sci., Vol. 822, New York (1997), pp. 284-302.
146. T. B. McCord, J. Morris, D. Persing, et al., *J. Geophys. Res.*, **100**, No. E2, 3245-3249 (1995).
147. E. L. Krinov, *Iron Shower* [in Russian], Moscow (1981).
148. E. L. Krinov and V. I. Tsvetkov, *Meteoritika*, Issue 38, 19-26 (1979).
149. V. I. Tsvetkov, *Meteoritika*, Issue 46, 3-10 (1987).
150. E. L. Krinov and S. S. Fonton, in: *Sikhote-Alin Iron Meteorite Shower* [in Russian], Vol. 1, Moscow (1959), pp. 157-303.
151. P. Farinella, P. Paolicchi, and V. Zappala, *Icarus*, **52**, 409-433 (1982).
152. A. Campo Bagatin, A. Cellino, D. R. Davies, et al., *Planet. Space Sci.*, **42**, 1079-1092 (1994).
153. P. Brown, A. R. Hilderband, D. W. E. Green, et al., *Meteoritics and Planet. Sci.*, **31**, 502-517 (1996).
154. D. O. ReVelle, R. W. Whitatter, and W. T. Normstrong, *Infrasound from the El Paso superbolide of October 9, 1997*, Los Alamos Nat. Lab. Report LA-UR-98-2893, Hanscom Air Force Base, Bedford, Mass. (1998).
155. W. W. Gibbs, *Scientific American*, November, 44-55 (1998).
156. I. V. Nemchinov (Nemtchinov), M. Yu. Kuz'micheva (Kuzmicheva), V. V. Shuvalov, et al., in: *IAU Colloquium 173*, Tatranská Lomnica (1998), p. 11.
157. A. J. Dessler, *Review of Geophysics*, **29**, 355-382 (1991).
158. M. Yu. Kuz'micheva (Kuzmitcheva), I. V. Nemchinov (Nemtchinov), O. P. Popova, and V. A. Rybakov, in: *Abstr. of Papers Submitted to the 26th Microsymp. on Comparative Planetology*, Moscow (1997), p. 72.
159. N. B. Divari, in: *Sikhote-Alin Iron Meteorite Shower* [in Russian], Vol. 1, Moscow (1959), pp. 26-48.
160. I. V. Nemchinov and V. V. Shuvalov, *Astron. Vestn.*, **26**, No. 4, 19-31 (1992).
161. I. V. Nemchinov (Nemtchinov) and V. V. Shuvalov, *Lunar and Planet. Sci.* (Houston), **XXIII**, 981-982 (1992).
162. A. V. Dobkin, T. V. Loseva, I. V. Nemchinov, et al., *Prikl. Mekh. Tekh. Fiz.*, No. 6, 35-45 (1993).
163. M. V. Boslough and D. A. Crawford, "*The Shoemaker–Levy 9 Impact Plumes on Jupiter: Implications for Threat to Satellites in Low-Earth Orbit*," in: Proc. of the Planetary Defense Workshop, Livermore, CA (1995).
164. I. V. Nemchinov (Nemtchinov) and T. V. Loseva, *Lunar and Planet. Sci.* (Houston), **XXV**, 987-988 (1994).
165. E. A. Gossard and W. Hook, *Waves in the Atmosphere*, Amsterdam (1975).
166. J. A. Hunt, R. Palmer, and W. Penney, *Phil. Trans. Roy. Soc.* (London), Ser. A, **352**, 275-315 (1960).
167. I. A. Nemchinov (Nemtchinov), A. A. Perelomova, and V. V. Shuvalov, *Lunar and Planet. Sci.* (Houston), **XXIV**, 1065-1066 (1998).

168. M. V. Boslough, D. A. Crawford, A. C. Robinson, and T. G. Trucano, *Geophys. Res. Lett.*, **21**, No. 14, 1555-1558 (1994).
169. D. A. Crawford (K. Noll, ed.), *Models of Fragment Penetration and Fireball Evolution. The Collision of Comet Shoemaker–Levy 9 with Jupiter* (1996).
170. K. Zahnle and M.-M. MacLow, *Icarus*, **108**, 1-17 (1994).
171. V. V. Shuvalov, *J. Geophys. Res.*, 3, No. E4, 5877-5890 (1999).
172. V. K. Gryaznov, B. A. Ivanov, A. B. Ivlev, et al., *Earth, Moon and Planets*, 66, 99-128 (1994).
173. B. A. Klumov, V. I. Kondaurov, A. V. Konyukhov, et al., *Usp. Fiz. Nauk*, **164**, No. 6, 617-630 (1994).
174. V. E. Fortov, Yu. N. Gnedin, M. F. Ivanov, et al., *Usp. Fiz. Nauk*, **166**, No. 4, 391-422 (1996).
175. M. B. E. Boslough and D. A. Crawford, in: J. L. Remo (ed.), *Near-Earth Objects*, Annals of the New York Acad. Sci., Vol. 822, New York (1997), pp. 236-282.
176. G. F. Plekhanov, A. F. Kovalevskii, V. K. Zhuravlev, and N. V. Vasil'ev, *Geolog. Geofiz.*, 6, 94-96 (1961).
177. K. G. Ivanov, *Meteoritika*, Issue 21, 46-48 (1961).
178. I. P. Pasechnik, in: *Space Matter on the Earth* [in Russian], Novosibirsk (1986), pp. 62-69.
179. L. A. Frank, J. B. Sigwarth, and J. D. Craven, *Geophys. Res. Lett.*, **13**, 303-306 (1986).
180. L. A. Frank, J. B. Sigwarth, and J. D. Craven, *Geophys. Res. Lett.*, **13**, 307-310 (1986).
181. L. A. Frank, J. B. Sigwarth, *Reviews of Geophys.*, **31**, 1-28 (1993).
182. L. A. Frank, J. B. Sigwarth, *Geophys. Res. Lett.*, **24**, 2427-2430 (1997).
183. M. B. E. Boslough and G. R. Gladstone, *Geophys. Res. Lett.*, **22**, No. 12, 1557-1560 (1995).
184. V. V. Shuvalov, N. A. Artem'eva (Artemieva), I. B. Kosarev, et al., *Lunar and Planet. Sci.* (Houston), **XXX**, 1045-1046 (1999).
185. G. R. Gladstone and M. B. E. Boslough, *EOS, Trans. Amer. Geophys. Union*, 1998 Spring Meeting, 79, No. 17, Paper SA31B-6, S238 (Supplement) (1998).
186. I. V. Nemchinov, I. B. Kosarev, M. Yu. Kuz'micheva (Kuz'mitcheva), et al., *EOS, Trans. Amer. Geophys. Union*, 1998 Spring Meeting, 79, No. 17, Paper SA31B-7, S238 (Supplement) (1998).
187. Z. Sekanina, P. W. Chodas, and D. K. Yeomans, *Astron. Astrophys.*, **289**, 607-636 (1944).
188. H. A. Weaver, M. F. A'Hearn, G. Arpigny, et al., *Science*, 267, 1282-1288 (1995).
189. H. B. Hammel, R. F. Beebe, A. P. Ingersoll, et al., *Science*, 267, 1288-1296 (1995).
190. P. A. Crawford, in: J. L. Remo (ed.), *Near-Earth Objects*, Annals of the New York Acad. Sci., Vol. 822, New York (1997), pp. 155-171.
191. G. Neukum, G. Hahn, T. Denk, et al., in: R. West and H. Bohnhardt (eds.), *European SL-9/Jupiter Workshop* ESO Headquarters, Garching bei München, Germany (1995), pp. 63-68.
192. K. Zahnle and M.-M. MacLow, *J. Geophys. Res.*, **100**, No. E8, 16885-16894 (1995).
193. B. A. Ivanov, I. V. Nemchinov (Nemtchinov), V. V. Svetsov, et al., *J. Geophys. Res.*, 97, 16167-16181 (1992).
194. I. V. Nemchinov (Nemtchinov), O. P. Popova, and R. E. Spalding, *Lunar and Planet. Sci.* (Houston), **XXIX**, 1272 (1998).
195. V. A. Rybakov, I. V. Nemchinov (Nemtchinov), V. V. Shuvalov, et al., *J. Geophys. Res.*, **102**, No. E4, 9211-9220 (1997).
196. T. J. Ahrens and A. W. Harris, in: T. Gehrels (ed.), *Hazards due to Comets and Asteroids*, Tucson and London (1994), pp. 897-927.
197. V. A. Simonenko, V. N. Nogin, D. V. Petrov, et al., in: T. Gehrels (ed.), *Hazards due to Comets and Asteroids*, Tucson and London (1994), pp. 929-953.
198. P. V. Plotnikov and L. V. Shurshalov, *Zh. Vych. Mat. Mat. Fiz.*, **34**, No. 1, 117-129 (1994).
199. P. V. Plotnikov and L. V. Shurshalov, *Zh. Vych. Mat. Mat. Fiz.*, 35, No. 8, 1233-1244 (1995).
200. P. V. Plotnikov and L. V. Shurshalov, *Zh. Vych. Mat. Mat. Fiz.*, **36**, No. 9, 120-123 (1996).
201. H. J. Melosh and I. V. Nemchinov (Nemtchinov), *Nature*, **366**, No. 6450, 21-22 (1993).
202. H. J. Melosh and I. V. Nemchinov (Nemtchinov), and Yu. I. Zetzer, in: T. Gehrels (ed.), *Hazards due to Comets and Asteroids*, Tucson and London (1994), pp. 1111-1132.
203. R. A. Alimov, E. V. Dmitriev, B. A. Ivanov, and I. V. Nemchinov (Nemtchinov), in: *Proc. of the Planetary Defense Workshop*, Livermore, CA (1995), pp. 465-469.
204. R. V. Alimov and E. V. Dmitriev, in: *Abstr. of Papers Submitted to the Int. Conf. "Asteroid Hazard-96"* [in Russian], St. Petersburg (1996), pp. 23-24.